1 **Title:** Metabolite exchange within the microbiome produces compounds that influence

2 *Drosophila* behavior

3

4 **Authors:** Caleb N. Fischer[1], Eric Trautman[2], Jason M. Crawford[2], Eric V. Stabb[3],

5 Nichole A. Broderick[1,4*], and Jo Handelsman[1]

6

7 **Affiliations:**

8 [1]Department of Molecular, Cellular and Developmental Biology, Yale University, New

9 Haven, CT, USA

10 [2]Department of Chemistry, Yale University, New Haven, CT, USA

11 [3]Department of Microbiology, University of Georgia, Athens, GA, USA

12 [4]Department of Molecular and Cell Biology, University of Connecticut, Storrs, CT, USA

13 *To whom correspondence should be addressed: E-mail: nichole.broderick@uconn.edu

14

15 **Abstract:**

16 Animals host multi-species microbial communities (microbiomes) whose

17 properties may result from inter-species interactions; however current understanding of

18 host-microbiome interactions is derived mostly from studies in which is it is difficult to

19 elucidate microbe-microbe interactions. In exploring how *Drosophila melanogaster*

20 acquires its microbiome, we found that a microbial community influences *Drosophila*

21 olfactory and egg-laying behaviors differently than individual members. *Drosophila*

22 prefers a *Saccharomyces-Acetobacter* co-culture to the same microorganisms grown

1

23 individually and then mixed, a response mainly due to the conserved olfactory receptor,

24 *Or42b. Acetobacter* metabolism of *Saccharomyces*-derived ethanol was necessary, and

25 acetate and its metabolic derivatives were sufficient, for co-culture preference.

26 Preference correlated with three emergent co-culture properties: ethanol catabolism, a

27 distinct volatile emission profile, and yeast population decline. We describe a molecular

28 mechanism by which a microbial community affects animal behavior. Our results

29 support a model whereby emergent metabolites signal *Drosophila* to acquire its

30 preferred multispecies microbiome.

31

32 **Introduction:**

33 Multispecies microbial communities (microbiomes) influence animal biology in

34 diverse ways (1): microbiomes modulate disease (2), metabolize nutrients (3),

35 synthesize vitamins (4), and modify behavior (5). A central goal in host-microbiome

36 studies is to understand the molecular mechanisms underpinning these diverse

37 microbiome functions.

38 Some aspects of microbial community function are the product of interspecies

39 interactions (6-9). For example, microorganisms modulate the metabolomes of

40 neighboring species (10) and microbial metabolites (e.g., antibiotics) alter bacterial

41 transcriptional responses (11). Despite current understanding of microbial inter-species

42 interactions *in vitro*, some of which has been elucidated in exquisite detail, the

43 consequences of microbial interspecies interactions within host-associated microbiomes

44 are just beginning to be explored experimentally.

45   Insight into host-associated microbiome function has stemmed mostly from

46   whole-microbiome (e.g., re-association of germ-free hosts with whole microbiomes (12))

47   and modeling microbiome function based on gene annotation (13) or single-

48   microorganism (e.g., re-association of germ-free hosts with a single microorganism

49   (14)) studies. However, these approaches tend to reveal only limited insight into

50   interspecies microbial interactions, which can provide hosts with essential services. For

51   example, termite symbionts carry genes necessary for metabolism of different parts of

52   complex carbohydrates (15), yet their function has not been demonstrated *in vivo*; co-

53   occurring human gut symbionts share polysaccharide breakdown products

54   cooperatively (16, 17), but the consequences of such interactions for the host are

55   unknown; inter-species bacterial interactions protect *Hydra* from fungal infection (18),

56   but the mechanism of host protection is unclear. The need to understand the effects of

57   inter-species microbiome interactions motivated our current work.

58   Attractive model systems in which to study the outcomes of inter-species

59   microbial interactions for host biology would include a tractable host that harbors a

60   simple multispecies microbiome. Here, we report the use of *Drosophila melanogaster* to

61   study interactions in a simple microbiome and their consequences for host behavior.

62   The *Drosophila* microbiome consists largely of yeasts, acetic acid bacteria, and

63   lactic acid bacteria (19-22). *Drosophila* ingests microbiome members from the

64   environment (e.g., fermenting fruit, (22-26)), a behavior posited as a mechanism for

65   *Drosophila* to select, acquire, and maintain its microbiome (21, 25). *Drosophila* behavior

66   toward environmental microorganisms has focused on yeasts (27-31). While yeasts

3

67   attract *Drosophila* via ester production (28, 29), lactic and acetic acid bacteria produce

68   metabolites (e.g., acids) that may repel *Drosophila*, based on olfactory avoidance of

69   high acid concentrations (32). One motivation of our study was to analyze *Drosophila*

70   behavior toward the yeast and bacteria that dominate the *Drosophila* microbiome.

71   Yeast and bacteria are largely studied within separate *Drosophila* sub-disciplines,

72   despite their shared habitat (21). Yeasts serve as food, providing *Drosophila* vitamins,

73   sterols, and amino acids (21). Lactic and acetic acid bacteria are gut microbiome

74   members (33) promoting larval development (34, 35), increasing resistance to

75   pathogens (25), inducing intestinal stem cell proliferation (36), and reducing adult sugar

76   and lipid levels (37, 38). Since microorganisms that are traditionally considered 'food'

77   co-exist with those considered "microbiome' in fruit fermentations and the two groups

78   provide *Drosophila* with different services, we hypothesized that *Drosophila* might detect

79   a beneficial community via metabolites that are produced cooperatively by the desirable

80   symbionts. Alternatively, *Drosophila* might detect a different metabolite as the signal for

81   each symbiont.

82   Fruit undergoes a well-characterized ripening process in which cell-wall

83   degrading enzymes and amylases convert the firm, starchy tissue into soft, sugar-rich

84   fruit (39-41). The high sugar content supports microbial colonization and fermentation

85   by *Drosophila*-associated microorganisms, including yeasts, lactic acid bacteria, and

86   acetic acid bacteria (23, 42). *Drosophila* avoids 'green' fruit and is attracted to 'overripe'

87   fruit (43), yet it is unclear whether *Drosophila* behavior is influenced by the fruit

88   microbiome and its metabolic properties. To this end, we developed a model fruit

4

89   fermentation system that afforded measurement of microbial populations, microbial

90   metabolites, and *Drosophila* behavior.

91   Here we demonstrate the importance of emergent microbiome metabolism—

92   quantitatively different or unique metabolites produced by the microbiome, but not by

93   any of its members in isolation—on behavior, suggesting that *Drosophila* modulates its

94   chemical intake by selecting a beneficial microbiome.

95

96   **Results:**

97   To determine whether *Drosophila* responds to emergent microbial community

98   metabolites, we used the T-maze olfactory assay to analyze *Drosophila* behavioral

99   responses to several *Drosophila* microbiome members grown individually or in

100   communities (Figure 1A, Table S1, Figure 1-figure supplement 1). When the strains

101   were grown individually, *Drosophila* was strongly attracted to yeasts, moderately

102   attracted to acetic acid bacteria, and neutral or slightly repelled by lactic acid bacteria

103   (Figure 1B, C). Because strains within a microbial group attracted *Drosophila* similarly, a

104   representative yeast, acetic acid bacterium, and lactic acid bacterium were used to test

105   the effect of interactions between microbiome members on *Drosophila* behavior.

106   *Drosophila* preferred microbial communities grown together to microorganisms grown

107   individually and then mixed prior to analysis (defined throughout as a separate-culture

108   mixture, Figure 1D). Focusing on a model *Saccharomyces cerevisiae* and *Acetobacter*

109   *malorum* community, we found that when tested against apple juice medium (AJM),

110   *Drosophila* preferred the community to the separate-culture mixture or individual

111   members (Figure 1E). In sum, *Drosophila* detects, and prefers, microorganisms growing

112   together to a mixture of the same strains combined after they had completed growth.

113   We next measured the attractiveness and other properties of the co-culture over

114   time. When grown alone, the microorganisms had similar growth profiles (Figure 2A).

115   However, when grown with *A. malorum, S. cerevisiae* populations first increased, then

116   decreased between 60 and 72 h, and were undetectable by 96 h (Figure 2A). The

117   decrease in *S. cerevisiae* viable counts mirrored a decrease in pH (Figure 2-figure

118   supplement 1A). *Drosophila* did not prefer the co-culture relative to the separate-culture

119   mixture at 34 h, slightly preferred the co-culture at 48 and 54 h, and strongly preferred

120   the co-culture at 60 through 96 h (Figure 2B). *Drosophila* preference for the co-culture

121   correlated with lower pH and *S. cerevisiae* populations, despite *Drosophila* olfactory

122   avoidance of acid (32) and reliance on yeast for nutrition (44) (Figure 2C, D). *Drosophila*

123   preference did not correlate with viable *A. malorum* populations (Figure 2- figure

124   supplement 1B). *Drosophila* preference for the co-culture increased relative to sterile

125   media during 34-96 h of growth, which is consistent with the increase in *Drosophila*

126   attraction being due to a property of the co-culture rather than to a decrease in

127   attraction to the separate-culture mixture (Figure 2-figure supplement 1C). In sum,

128   several properties of the microbial community (e.g. *S. cerevisiae* density, pH) parallel

129   *Drosophila* detection of, and preference for, the co-culture.

130   Mutants in broadly and narrowly tuned ionotropic and olfactory receptors (Irs and

131   Ors, respectively, (45, 46)) were used to evaluate the role of *Drosophila* olfactory

132   reception in discriminating the co-culture from the separate-culture mixture during and

6

133   immediately following peak attraction (Figure 3-figure supplement 1). During the most

134   attractive phase of the co-culture (e.g. 67-115 h), Or83b and Or42b showed significant

135   attraction to the co-culture, whereas no role was detected for Irs or Or35a (Figure 3). As

136   the co-culture proceeded (e.g. 139-163 h), attraction decreased and the role of Or42b

137   and Or83b waned (Figure 3). Or83b is a required co-receptor for all other Or gene

138   products (47) and Or42b, one of the most conserved olfactory receptors, detects esters

139   and 1,1-diethoxyethane (48-50).These results suggest that Or42b enables *Drosophila* to

140   distinguish the co-culture from the separate-culture mixture. Our results suggest that a

141   non-Or83b factor explains ~40% of *Drosophila* co-culture preference (Figure 3).

142   Previous work found that Or83b is fully responsible for *Drosophila* attraction to apple

143   cider vinegar (51), suggesting that the behavioral circuit activated by inter-species

144   interactions of the co-culture is distinct from the circuit activated by apple cider vinegar.

145   We speculated that the emergent property of co-culture attractiveness might

146   arise from a distinct metabolic profile of the co-culture. Using gas chromatography-mass

147   spectrometry (GC-MS), we identified volatiles unique to or differentially produced in the

148   co-culture compared to the separate-culture mixture. Five co-culture volatiles (ethanol,

149   isobutanol, isoamyl alcohol, acetic acid, isoamyl acetate) were confirmed with standards

150   (Table 1-figure supplements 1-2) and quantified with standard curves (Table 1-figure

151   supplement 3). The alcohol concentrations were lower, and acetic acid and isoamyl

152   acetate were unique in the co-culture relative to the other experimental groups (Table

153   1). The molecular profile was reminiscent of ethanol catabolism as the unique co-culture

154   metabolic process. We therefore hypothesized that ethanol catabolism was the

155   emergent metabolic process.

156   We next measured ethanol and acetic acid levels over time (24-156 h) and

157   compared the chemical dynamics to *Drosophila* preference. Consistent with a

158   relationship between ethanol catabolism, acetic acid anabolism, and *Drosophila*

159   attraction, ethanol levels declined and acetic acid accumulated in the co-culture at a

160   similar time of *Drosophila* co-culture preference (Figure 4A). Furthermore, as ethanol

161   catabolism and acetic acid anabolism proceeded (36-96 h), *Drosophila* attraction toward

162   the co-culture increased until 96 h, at which point it decreased, consistent with lower

163   turnover of ethanol at the end of ethanol catabolism (Figure 4A, black line).

164   We hypothesized that *Drosophila* preferred the community during peak ethanol

165   turnover (e.g. co-cultures at ~72 h of growth) compared with the community pre-ethanol

166   catabolism (e.g. co-culture at ~36 h of growth) or during late-stage ethanol catabolism,

167   in which ethanol turnover is low (e.g. co-culture at ~144 h of growth; Figure 4A).

168   Consistent with our hypothesis, *Drosophila* preferred the co-culture in the middle stage

169   of ethanol catabolism to earlier or later stages of ethanol catabolism (Figure 4B).

170   We hypothesized that *Drosophila* preference for communities during peak

171   ethanol turnover reflected fitness benefits derived from ingesting metabolites associated

172   with different staged communities. To test this hypothesis, we measured *Drosophila*

173   survival when given ethanol and acetic acid concentrations characteristic of microbial

174   cultures at different stages of ethanol catabolism. *Drosophila* survival was highest when

175   given metabolites associated with middle-staged ethanol catabolism compared with pre-

8

176   or end-stage ethanol catabolism (Figure 4C). In sum, our results are consistent with

177   *Drosophila* preference providing benefits associated with consumption of microbial

178   community-generated metabolites.

179   To test directly whether ethanol catabolism underpinned *Drosophila* co-culture

180   preference, we evaluated *Drosophila* preference for the co-culture harboring a mutant in

181   *adhA*, which encodes pyrroloquinoline quinone-dependent alcohol dehydrogenase

182   (PQQ-ADH-I), the enzyme that converts yeast-derived ethanol into acetaldehyde on

183   path to acetic acid (34). Co-cultures using either *A. malorum* or *A. pomorum* wild-type

184   (WT) along with *S. cerevisiae* were equally attractive to *Drosophila* (Figure 5-figure

185   supplement 1). *Drosophila* preferred the co-culture containing *A. pomorum* WT versus a

186   separate-culture mixture; however, *Drosophila* did not prefer the co-culture containing

187   *A. pomorum adhA* versus a separate-culture mixture (Figure 5A), suggesting that

188   ethanol catabolism is necessary for *Drosophila* to discriminate between the two

189   conditions. *Drosophila* preferred the co-culture containing *A. pomorum* WT to the co-

190   culture containing *A. pomorum adhA* (Fig. 5A). Moreover, *Drosophila* preferred to lay

191   eggs in the co-culture containing *A. pomorum* WT to the co-culture containing *A.*

192   *pomorum adhA*, further substantiating the importance of ethanol catabolism in

193   *Drosophila* biology, as egg-laying decisions are crucial to reproductive success (Figure

194   5B).

195   We next identified additional metabolites unique to the co-culture using solid-

196   phase microextraction gas chromatography-mass spectrometry (SPME GC-MS). Acetic

197   acid, six acetate esters, an acetaldehyde metabolic derivative (acetoin), a putative

198   acetaldehyde metabolic derivative (2,4,5-trimethyl-1,3-dioxolane), and two unknown

199   metabolites were more abundant in the co-culture relative to the separate-culture

200   mixture or co-culture with *A. pomorum* lacking *adhA* (Table 2, Table 2- figure

201   supplements 1-2). To determine the molecular basis for *Drosophila* co-culture

202   preference, select metabolites were added to the co-culture containing *A. pomorum*

203   *adhA*. Esters and acetic acid, but not esters alone, were sufficient to fully restore *A.*

204   *pomorum adhA* attractiveness to *A. pomorum* WT levels (Figure 5A).

205   Although acetate and its metabolic derivatives were sufficient for *Drosophila* co-

206   culture preference, acetaldehyde is a reactive intermediate during ethanol catabolism

207   whose metabolic derivatives might be increased in microbial communities compared

208   with individual microbial cultures. Consistent with this idea, acetoin was moderately

209   increased in the co-culture compared with the separate-culture mixture (Table 2-figure

210   supplement 1); strikingly, acetoin was increased ~27-fold in the tri-culture (*S. cerevisiae*,

211   *A. malorum*, and *L. plantarum*) compared to the co-culture (Figure 6A, B, Figure 6-

212   figure supplement 1) and was attractive to *Drosophila* (Figure 6-figure supplement 2). In

213   sum, emergent metabolites from 2- and 3-membered communities, including

214   acetaldehyde metabolic derivatives, attract *Drosophila*.

215   To investigate further the potential role of acetaldehyde and its metabolic

216   derivatives in *Drosophila* behavior, we performed a dose response in which

217   acetaldehyde was added to the separate-culture mixture (Figure 6-figure supplement

218   3A) to evaluate its ability to induce attractiveness to co-culture levels. Even at the lowest

219   tested levels, acetaldehyde supplementation stimulated the separate-culture mixture to

10

220   attractiveness levels equal to the co-culture (Figure 6-figure supplement 3A); moreover,

221   acetaldehyde and its metabolic derivatives 'over-restored' preference of the separate-

222   culture mixture beyond WT co-culture levels at its most attractive dose (Figure 6- figure

223   supplement 3A). Finally, three acetaldehyde metabolic derivatives—acetoin, 1,1-

224   diethoxyethane (an acetal), and 2,3-butanedione—were sufficient to induce the

225   attractiveness of the separate-culture mixture to WT co-culture levels using

226   concentrations of each metabolite at or below the physiological concentration of acetoin

227   found in the tri-culture (Figure 6-figure supplement 3B). Creating a pure metabolite

228   mixture comprised of key metabolic groups produced by microbial communities and

229   identified in this study (esters, acetaldehyde metabolic derivatives, alcohols, acid)

230   attracted *Drosophila* similarly to the co-culture (Figure 6-figure supplement 4A, B).

231   Interestingly, the acetaldehyde metabolic derivatives alone were sufficient and the most

232   attractive (Figure 6- figure supplement 4C, D), supporting acetaldehyde metabolic

233   derivatives as potent *Drosophila* attractants.

234   Overall, our results suggest that both esters and acetaldehyde metabolic

235   derivatives are keystone microbial community metabolites that attract *Drosophila*. We

236   next created a simple 9-metabolite mixture in water (containing only 1 acid, 4 esters,

237   and 4 acetaldehyde metabolic derivatives) and measured *Drosophila* preference toward

238   this mixture in relation to the yeast-acetic acid bacteria co-culture, the yeast-acetic acid

239   bacteria-lactic acid bacteria microbial community, or apple cider vinegar (ACV). The

240   defined mixture used concentrations for each acetaldehyde metabolic derivative similar

241   to the concentration of acetoin in the tri-culture and ester and acid concentrations that

242   were in the range of detected in the co-culture. The defined 9-metabolite mixture was

243   more attractive than all other conditions (Figure 6- figure supplement 5). In sum,

244   acetaldehyde metabolic derivatives and esters are potent *Drosophila* attractants whose

245   detection may signal the presence of actively metabolizing, multispecies microbial

246   communities.

247

248   **Discussion:**

249   Here, we have demonstrated how emergent properties of a microbial

250   community—volatile profile, population dynamics, and pH—influence *Drosophila*

251   attraction, survival, and egg-laying behaviors. Our study is the first to identify the

252   consequences of microbe-microbe metabolic exchange on animal behavior and

253   discovers additional microbial interactions for further mechanistic study (Figure 1D).

254   Microbe-microbe metabolic exchange generates unique and quantitatively

255   different volatiles from those resulting from individual microbial metabolism (Tables 1 &

256   2, Figure 7). *Acetobacter*-generated acetate coupled to *Saccharomyces*-derived

257   alcohols spawn diverse acetate esters (Table 1 & Table 2). We hypothesize that more

258   complex and diverse communities, comprising alcohol-producing yeasts, acetate-

259   producing *Acetobacter*, and lactate-producing *Lactobacillus*, will generate a wider array

260   of attractive esters (Figure 7). The community of *S. cerevisiae*, *A. malorum*, and *L.*

261   *plantarum* emitted higher levels of acetoin and attracted *Drosophila* more strongly than

262   the co-culture of *S. cerevisiae* and *A. malorum* (Figure 1D, Figure 6). Acetoin and 2,3-

263   butanedione are formed by an α-acetolactate intermediate in bacteria and directly from

12

264 acetaldehyde in yeast (52). We therefore hypothesize that communities of yeasts and

265 bacteria may emit high levels of attractive acetaldehyde metabolic derivatives (Figure

266 7).

267 *Drosophila* behavioral studies have mostly focused on yeasts, even though

268 *Drosophila* evolved in a bacterial-rich environment. Our results suggest that non-yeast

269 microorganisms, especially when grown in microbial communities, affect *Drosophila*

270 behaviors. We reason that additional investigations that couple chemical microbial

271 ecology with *Drosophila* behavior will herald the discovery of microbe-influenced

272 behaviors and microbial community-generated metabolites.

273 This study demonstrates the coordination of ethanol synthesis and catabolism by

274 *S. cerevisiae* and *Acetobacter,* respectively, and the role of ethanol in *Drosophila*

275 behavior and survival. Non-*Saccharomyces Drosophila* microbiome members also

276 make ethanol (53) and diverse acetic acid bacteria catabolize ethanol, generalizing our

277 findings to other microbial community combinations. Ethanol can have deleterious or

278 beneficial fitness consequences for *Drosophila* depending on concentration (54, 55) and

279 ecological context (56). Our results show that *Drosophila* uses products of inter-species

280 microbiome metabolism to detect a community that titrates ethanol concentration

281 optimally for the host. Work that further dissects the consequences of acetic acid and

282 ethanol concentrations on *Drosophila* biology and investigates other community-level

283 metabolic profiles will be of interest to enrich the chemical and ecological portrait of the

284 *Drosophila* microbiome.

285   Our work raises questions about the consequences of the observed behavior on

286   microbiome assembly and stability in the *Drosophila* intestine. *Drosophila* possesses

287   specific and regionalized gut immune responses to the microbiome (57-60) implying a

288   tolerant environment in which privileged microbiome members are maintained and

289   reproduce in the *Drosophila* intestine. Other work suggests that *Drosophila* acquires its

290   adult microbiome from exogenous sources, that adult microbiome abundance drops

291   without continuous ingestion of exogenous microorganisms, and that the microbiome

292   can be shaped by diet (19, 25, 26). As such, a combination of internal mechanisms,

293   exogenous factors, and host behavior likely sculpt the microbiome; determining the

294   relative contribution of each will be important moving forward. Complicating our

295   understanding of the contribution of these factors is the opaque distinction between

296   'microbiome' and 'food', since both are ingested from the environment (61). To dissect

297   the formation and stability of the *Drosophila* microbiome, the fate of ingested

298   microorganisms needs to be monitored and microbial intestinal reproduction needs to

299   be surveyed as a function of *Drosophila* behavior, age, immune status, microbiome

300   membership, and nutritional state (e.g. using synthetic diets without yeast; (34, 62)).

301   In sum, our results support a model in which the *Drosophila* olfactory system is

302   tuned to fruity (e.g., esters) and buttery (several acetaldehyde metabolic derivatives,

303   such as 2,3-butanedione) smelling metabolites promoted by microbe-microbe

304   interactions. We anticipate that accounting for microbial interactions in diverse host-

305   microbe studies will lead to new insights into diverse aspects of microbial-animal
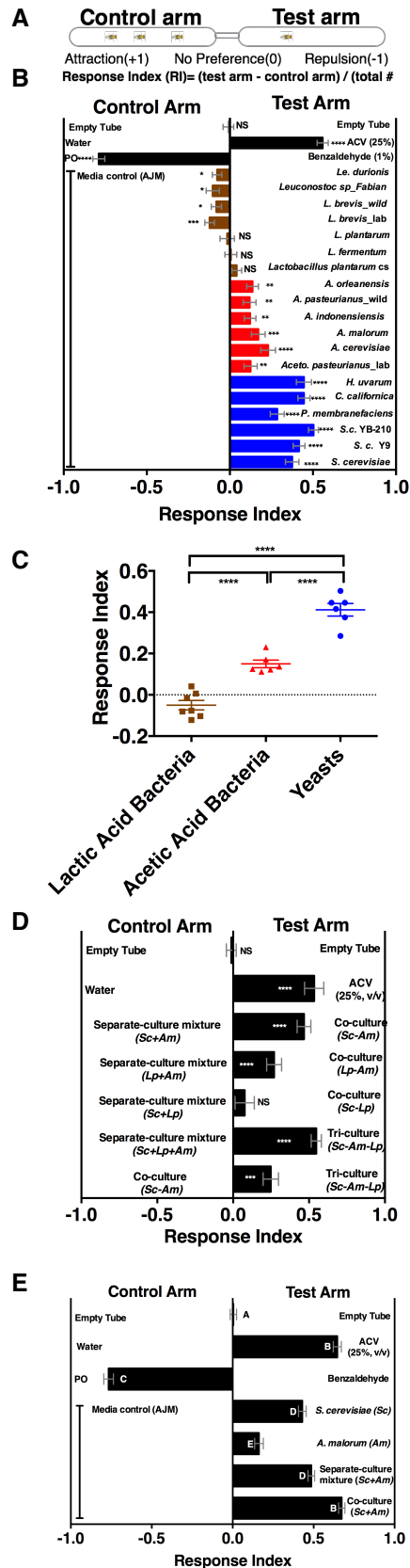
306   symbioses.

14

324

Fig. 1. *Drosophila* detection of microbe-microbe metabolic exchange. **(A)** T-maze setup and quantification. **(B)** *Drosophila* behavior toward yeasts (blue), acetic acid bacteria (red), and lactic acid bacteria (brown) (Table S1). Mean ± SEM of 12-36 replicates (n=2-6 experiments). Each T-maze replicate uses a technical replicate of a microbial culture and one cohort of *Drosophila* maintained in separate vials for 3-5 days. Mock (two empty tubes), ACV (25% apple cider vinegar versus water), and benzaldehyde (1% versus paraffin oil (PO)). A one-sample t-test assessed deviance from 0. Symbols: NS p >0.05; * p ≤0.05; ** p ≤0.01; *** p ≤0.001; **** p ≤0.0001. **(C)** Mean *Drosophila* behavior toward each microorganisms was graphed according to microbial group and analyzed by one-way ANOVA. **(D)** *Drosophila* behavior toward community combinations of a representative yeast, acetic acid bacterium, and lactic acid bacterium in relation to their separate-culture mixture (grown individually and mixed; *Sc = S. cerevisiae*; *Am= A. malorum; Lp = L. plantarum* cs) grown for 96 h; *Drosophila* preference for the three- versus two-membered community is the last column. Mean ± SEM of 12-18 replicates (n=2-3 experiments). A one-sample t-test assessed deviance from 0. **(E)** *Drosophila* olfactory behavior toward the *S. cerevisiae* and *A. malorum* community and its constituent parts relative to media grown for 48-60 h. Mean ± SEM of 18-30 replicates (n=5 experiments). Differences between groups were assessed by ANOVA. A Tukey's multiple comparison test was used to assess significant differences between groups (p≤0.05), as indicated by unique letters.
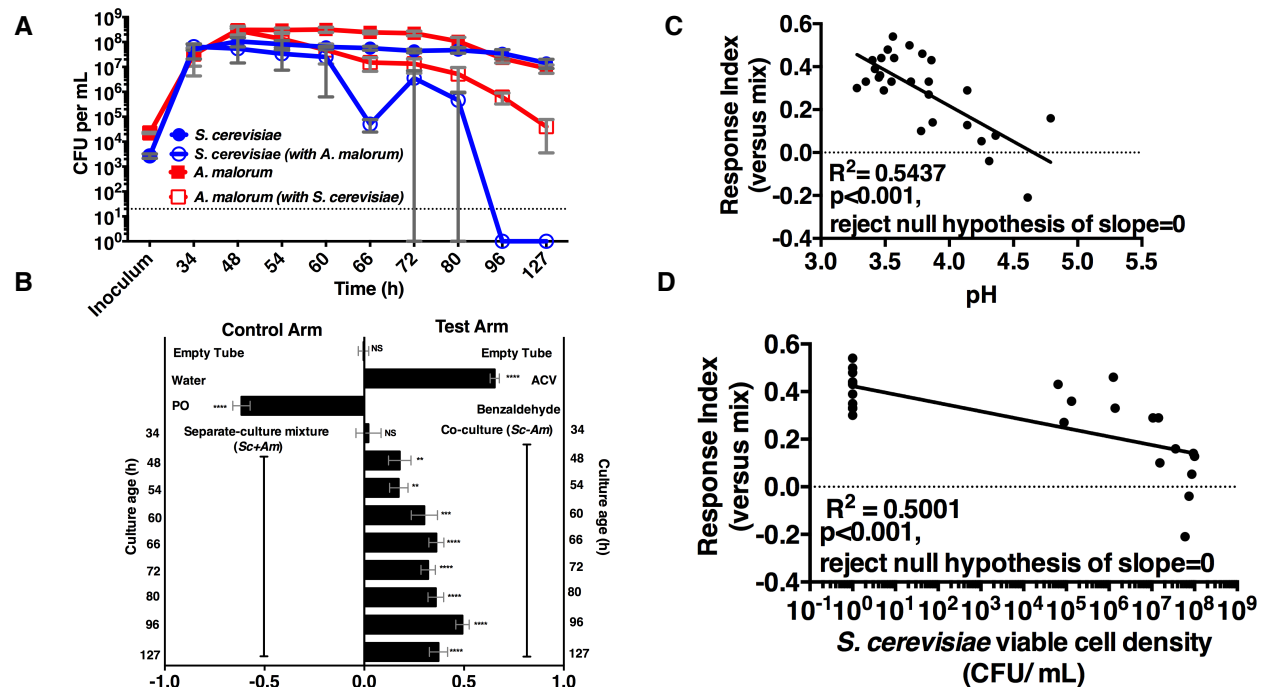
16

Fig. 2. *Drosophila* temporal preference for metabolic exchange. **(A)** *S. cerevisiae* and *A. malorum* viable populations. Mean ± SEM of 2-3 experiments with one pooled replicate (2-3 cultures derived from the same colony) per experiment. Limit of detection is 20 CFU/mL. **(B)** *Drosophila* olfactory behavior toward co-cultured *S. cerevisiae* and *A. malorum* versus its separate-culture mixture as a function of culture age. Mean ± SEM of 16-18 replicates from three experiments. A t-test against a hypothetical value of zero assessed deviance from 0. Symbols: NS p >0.05; * p ≤0.05; ** p ≤0.01; *** p ≤0.001; **** p ≤0.0001. **(C)** Relationship between pH and *Drosophila* preference for the *S. cerevisiae* and *A. malorum* co-culture versus the separate-culture mixture. Each data point represents the pH of a co-culture and the mean RI of *Drosophila* toward the same co-culture. A linear standard curve with an unconstrained slope was generated and compared to a null model with slope=0. The data fit to an unconstrained slope better than to the null model (p<0.0001, slope = -0.3295). **(D)** Relationship between *S. cerevisiae* populations and *Drosophila* preference for the co-culture versus the separate-culture mixture. Each data point represents viable *S. cerevisiae* populations of the culture along with the mean RI value toward the co-culture containing *S. cerevisiae*. A semilog standard curve with an unconstrained slope was generated and compared to a null model with slope=0. The data fit to an unconstrained slope better than to the null model (p<0.0001, slope = -0.0349).

17
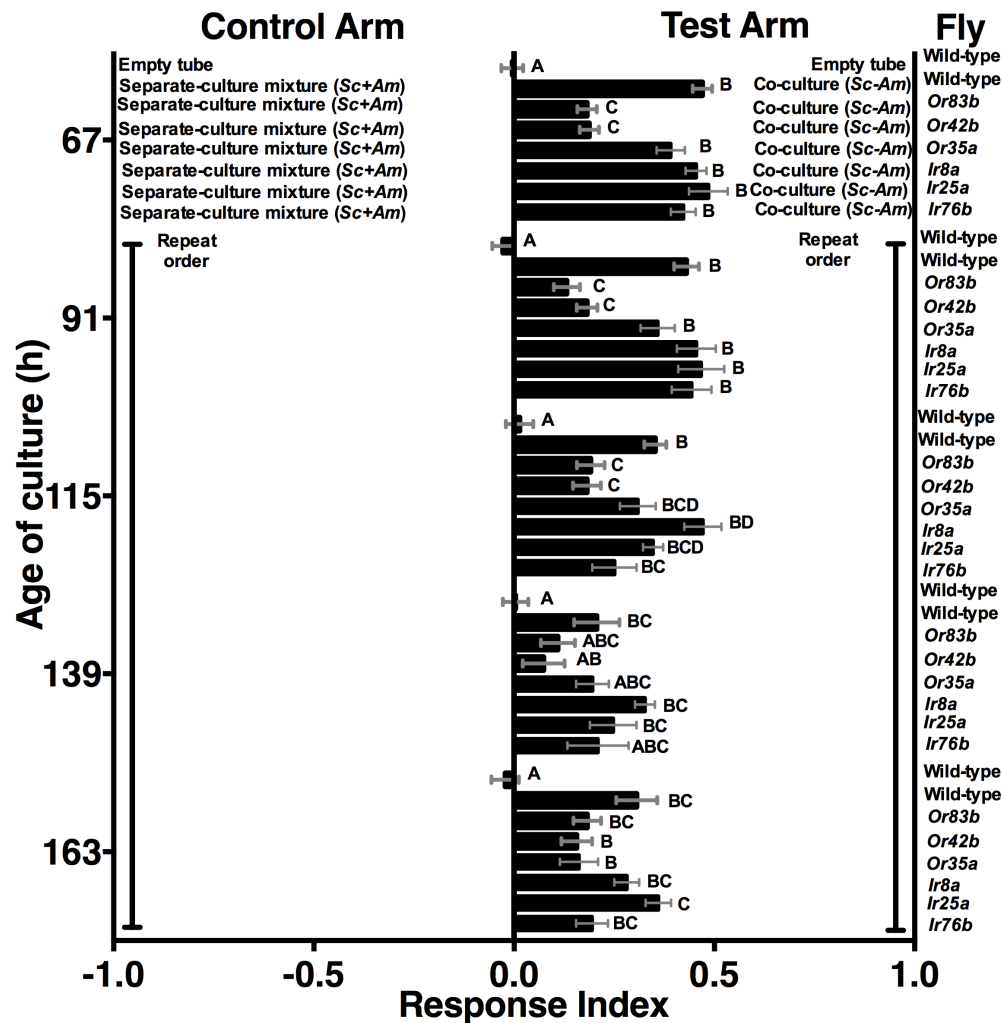
Fig. 3. Role of olfactory receptor mutants in *Drosophila* detection of inter-species microbial interactions. Culture were grown at and after peak *Drosophila* attraction. Differences were assessed by a one-way ANOVA within each culture age. A Tukey's multiple comparison test was used to assess significant differences between groups (p≤0.05), as indicated by unique letters. Mean +/- SEM of 12-24 replicates per time point per fly condition (n=2-4 experiments per time point).

18

Fig. 4 *Drosophila* behavior, survival, and ethanol catabolism. **A)** Dynamics of ethanol, acetic acid and *Drosophila* co-culture preference. Acetic acid was only detected in the co-culture. The abundance was derived from a linear regression calculated from standards (figs. S6). Chemical data is the mean ± SEM of two values calculated from two experiments with th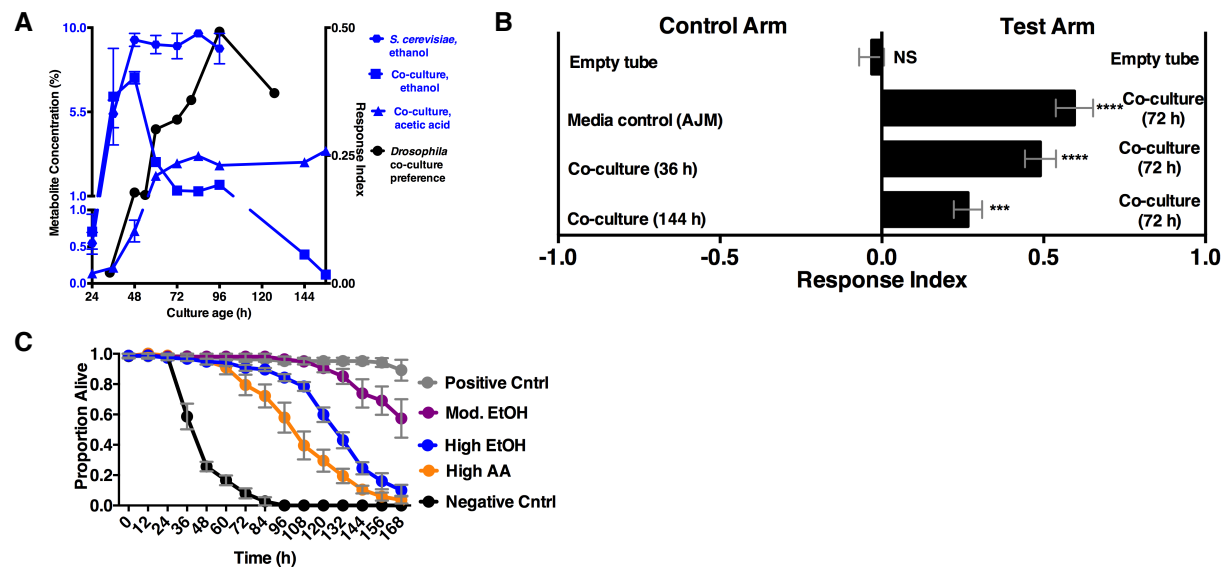ree replicates per experiment (except acetic acid and ethanol concentrations at 144 and 156 h, which are from one experiment with three replicates). *Drosophila* co-culture preference is the mean value of the preference shown in Figure 2B. **B)** *Drosophila* preference for stages of ethanol catabolism. 72 h is 'mid' stage; 36 h is 'early' stage and 144 is 'late' stage. The co-culture contains *S. cerevisiae* and *A. malorum* grown for the time indicated. AJM= apple juice media. Data points represent the mean ± SEM of the combined results of two experiments with 8-10 total replicates per group. A t-test assessed whether the values were different from zero. C) *Drosophila* survival in the presence of acetic acid (AA), ethanol (EtOH) or the combination of the two in water. Groupings were based on concentrations of metabolites estimated from pre-ethanol catabolism (9.4% ethanol, High EtOH), middle-staged ethanol catabolism (1.4% ethanol, 2.8% acetic acid, Mod. EtOH) and post ethanol catabolism (3.42% acetic acid, High AA). Data represent mean +/- SEM of 5-6 replicates of one representative experiment of two. Mod. EtOH was significantly different from High EtOH condition from 108 h onward and High AA condition from 72 h onward (assessed by two-way ANOVA comparing time and condition, p≤0.05, Tukey's correction). Negative Cntrl is water and Positive Cntrl is Shield's & Sang M3 Insect Medium.

432 **A**

439 **Response Index**

440 **B**
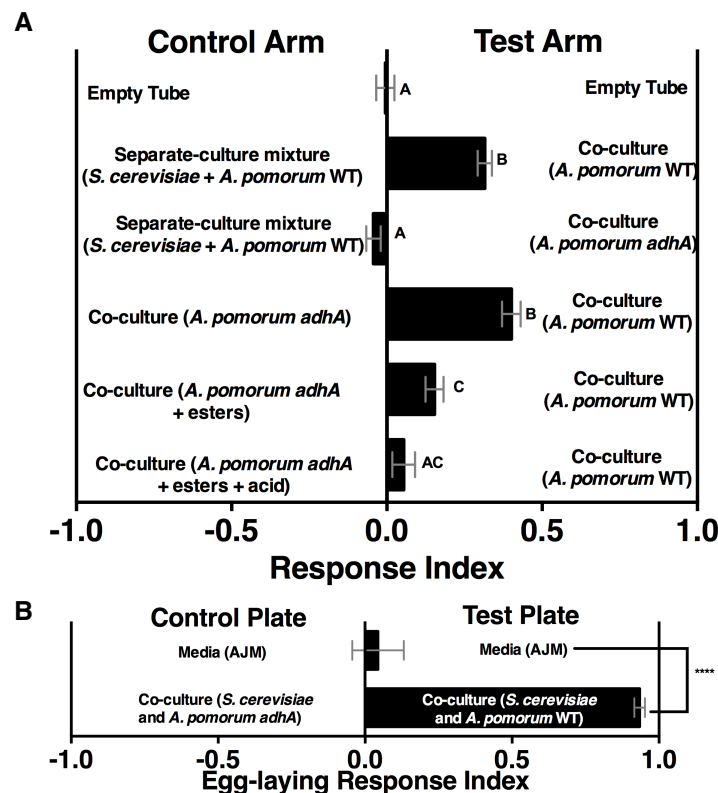
Fig. 5. Role of ethanol catabolism in *Drosophila* olfactory and egg-laying behaviors. **(A)** *Drosophila* olfactory behavior toward specified conditions. Mean ± SEM of 2-7 experiments with 10-42 total replicates. Differences were assessed by a one-way ANOVA. A Tukey's multiple comparison test was used to assess significant differences between groups (p≤0.05), as indicated by unique letters. Esters include ethyl acetate, isoamyl acetate, 2-phenethyl acetate, isobutyl acetate, 2-methylbutyl acetate, and methyl acetate; acid is acetic acid. Amounts added are based on physiological amounts in co-cultures and are found in Table 2. The co-culture contains *S. cerevisiae* and the specified *A. pomorum* strain. acid= acetic acid **(B)** *Drosophila* was given a choice to lay eggs in a co-culture containing *S. cerevisiae* and *A. pomorum* wild-type (WT) or *S. cerevisiae* and *A. pomorum adhA*. The co-cultures were grown for 96 h and mixed 1:1 with a 1.6% agarose solution. *Drosophila* was allowed to lay eggs for eight hours. Difference between the two groups was assessed by an unpaired t-test (**** p≤0.0001). Mean ± SEM of 16-18 replicates from two experiments.

20

457
458
459
460
461
462
463
464
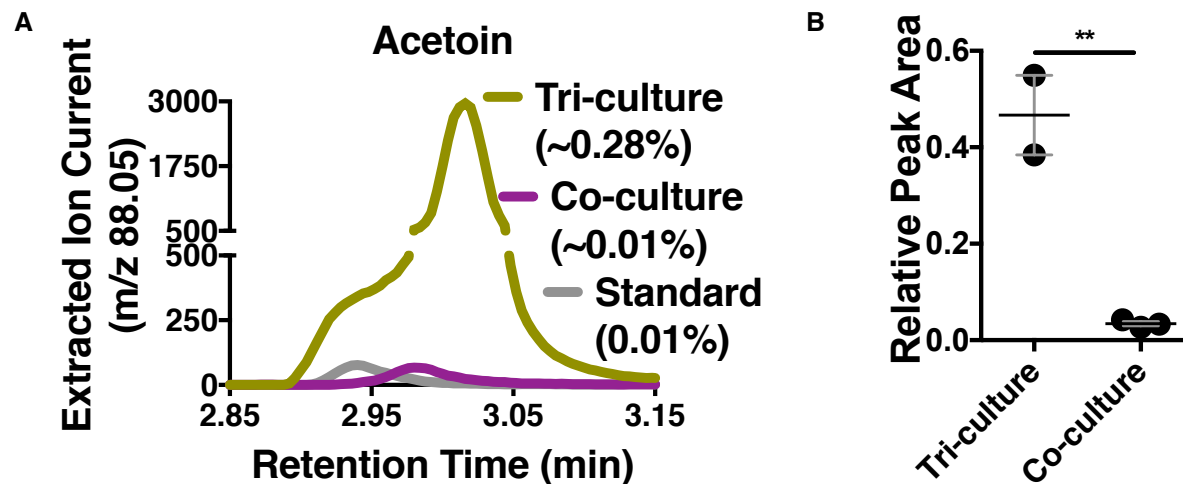
465 **Fig. 6.** Acetoin as an attractive metabolite increased in the 3-membered communitiys **A)** Representative

466 chromatogram of the tri-culture (*S. cerevisiae-A. malorum-L. plantarum*) compared to the co-culture (*S.*

467 *cerevisiae* and *A. malorum*). **B)** Estimated quantification of is based on a linear regression of acetoin

468 (figure 6-figure supplement 1). Relative quantification of acetoin in the tri-culture (one replicate with *A.*

469 *malorum* and one replicate with *A. pomorum* from separate days) and the co-culture (one replicate with *A.*

470 *malorum* and two replicates with *A. pomorum* from separate days). Difference in peak areas was

471 assessed by an unpaired two-tailed t-test (** p≤0.01).

472
473
474
475
476
477
478
479
480
481

21
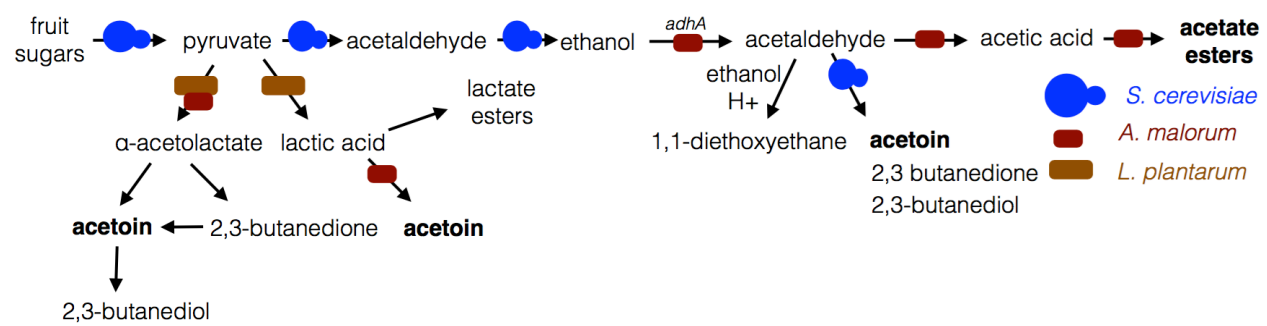
Figure 7. Model of microbe-microbe metabolite exchange. Bolded are metabolites increased due to microbe-microbe interactions.

509 **Table 1.** Summary of volatiles detected using GC-MS

Identity	Standard confirmation	Relative quantification (co-culture: separate-culture mixture)
Ethanol	Y	5.0-12.6-fold reduced
Isobutanol	Y	7.3-24.7-fold reduced
Isoamyl acetate	Y	unique to co-culture
Isoamyl alcohol	Y	3.6-6.4-fold reduced
Acetic acid	Y	unique to co-culture

510 **Table 1.** Relative abundance of volatiles in the co-culture (*S. cerevisiae* and *A. malorum* grown together)

511 compared to the separate-culture mixture (*S. cerevisiae* and *A. malorum* grown separately, and their

512 quantities added in during anaylsis). GC-MS captured volatiles with XAD-4 beads suspended above the

513 cultures during growth; subsequently, beads were methanol-extracted (n=6 experiments, Table 1-figure

514 supplements 1-2). Quantification is based on two experiments in which a linear regression was computed

515 with standards (Table 1-figure supplement 3). Quantification is based on beads suspended above the

516 cultures between 84 and 96 h of culture growth.

517

518

519

520

521

522

523

524

525

526

527

528

529

530 **Table 2.** Estimated concentrations of key metabolites in the co-culture using SPME GC-MS

Metabolite	Lin. reg. eq. 1	Lin. reg. eq. 2	Normalized Peak Area (single experiment)	Normalized Peak Area (Average, All experiments)	Estimated Concentration (%)
Isobutyl acetate	Y=4151X - 0.1319	Y=3252X - 0.07251	0.29	1.16	0.00023
Isoamyl acetate	y=8158X	Y = 7800X	0.78	3.8	0.00026
2-Phenethyl acetate	Y=5129X -0.04011	Y=6972X -0.2013	1.2	1.9	0.00028
2-Methylbutyl acetate	Y=8995X - 0.05042	Y=8087X-0.1307	0.56	3.1	0.00023
Methyl acetate	Y=75.22X +0.004457	NA	0.018	0.040	0.00033
Ethyl acetate	NA	NA	NA	NA	~0.02*
Acetic acid	NA	NA	NA	NA	~3.0*
Acetoin	NA	NA	NA	NA	~0.01*

531 **Table 2.** Estimated concentrations of differentially concentrated or unique metabolites in the co-culture.

532 Linear regression equations (Lin. reg. eqs. 1 and 2) were estimated from individual experiments in which

533 peak areas of different concentrations of metabolites were fitted with a linear regression (Table 2-figure

534 supplement 2). Normalized peak areas correspond to the specified metabolites in co-cultures containing

535 *S. cerevisiae* and *A. malorum*. Separate estimates were derived from a normalized peak area estimated

536 from a single experiment (co-culture and standard samples were from a run with similar internal standard

537 signal) or from the mean normalized peak area estimated from all experiments (co-cultures were run over

538 four days, standards were run on two days). The final estimated concentration was an average of all

539 estimated concentrations (n=4 estimates (two from each standard regression equation times two

540 estimates of the normalized peak area), execpt for methyl acetate, n=2 estimates). The estimated

541 concentrations (exept acetoin) were added to the co-culture containing *A. pomorum adhA* (Figure 5A).

542 *Ethyl acetate, acetic acid and acetoin concentrations were estimated from standards in Table 2-figure

543 supplement 1.

544

545

546

547

548

24

549 **SUPPLEMENTARY MATERIALS**

Table S1. Microorganisms and their sources used in this study

Organism	Clade	Source
Saccharomyces cerevisiae	Yeast	*Drosophila pinicola,* Phaff culture collection
S. cerevisiae Y9	Yeast	Ragi (similar to Sake wine) fermentation (30)
S. cerevisiae YB-210	Yeast	Banana; ARSC culture collection (63)
Pichia membranefaciens	Yeast	*D. melanogaster* in Handelsman Laboratory
Candida californica	Yeast	Bananas and *D. melanogaster* habitat in Stamps laboratory; Phaff culture collection
Hanseniaspora uvarum	Yeast	Bananas and *D. melanogaster* habitat in Stamps laboratory; Phaff culture collection
Lactobacillus plantarum cs	LAB	*D. melanogaster* in Handelsman Laboratory (25)
*L. brevis*_lab	LAB	*D. melanogaster* in Handelsman Laboratory
L. fermentum	LAB	*D. melanogaster* in Handelsman Laboratory
*L. brevis*_wild	LAB	Wild-caught *D. melanogaster* (19)
Leuconostoc sp_Fabian	LAB	Wild-caught *D. melanogaster* (64)
L. plantarum	LAB	*D. melanogaster* in Handelsman Laboratory
Leuconostoc durionis	LAB	Wild-caught *D. melanogaster* (64)
*Acetobacter pasteurianus*_lab	AAB	*D. melanogaster* in Handelsman Laboratory
A. cerevisiae	AAB	*D. melanogaster* in Handelsman Laboratory
A. malorum	AAB	*D. melanogaster* in Handelsman Laboratory
A. indonensiensis	AAB	*D. melanogaster* in Handelsman Laboratory
*A. pasteurianus*_wild	AAB	Wild-caught *D. melanogaster* (19)
A. orleanensis	AAB	Wild-caught *D. melanogaster* (19)
A. pomorum	AAB	*D. melanogaster* in Won-Jae Lee Laboratory (34)
A. pomorum adhA	AAB	Mutant derivative of *A. pomorum* (34)

550 LAB = lactic acid bacteria; AAB = acetic acid bacteria

25
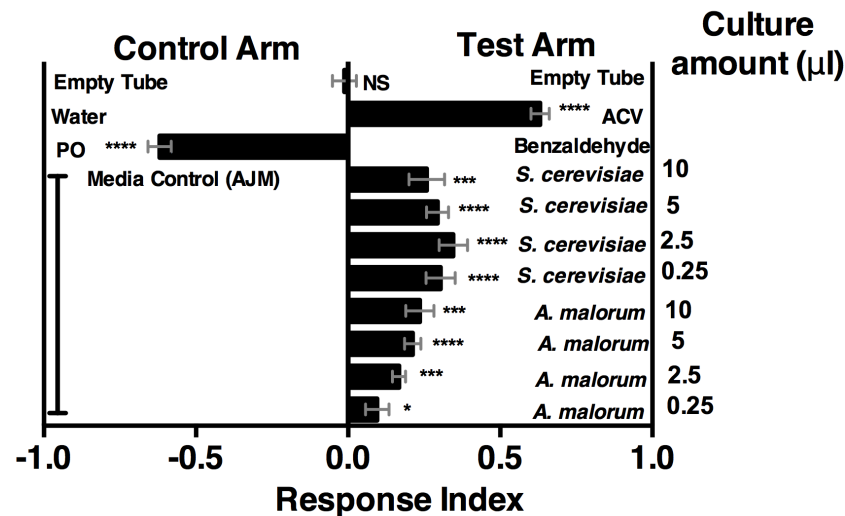
Figure 1-figure supplement 1. *Drosophila melanogaster* olfactory behavior toward different culture volumes of *Saccharomyces cerevisiae* and *Acetobacter malorum*. The top three experimental groups are controls: Mock (empty tube versus empty tube) recapitulates alternating of test and control arms, as in all experimental groups; apple cider vinegar (ACV (25% in water)) is the positive control and tested against water only; Benzaldehyde (1%) is the negative control and is a 100-fold dilution of benzaldehyde in paraffin oil (PO) tested against paraffin oil only. In all experimental groups, 10μl of total volume was used; the culture amount is specified, when appropriate, on the right-hand portion of the plot. The remaining volume in the microbial groups is water. Media control (AJM) is always 5μl of AJM mixed with 5μl of water. Data points represent the mean +/- SEM combined from three experiments (n=12 per experimental group). A t-test was performed against a hypothetical value of 0 to test for significance and is denoted by the following system (consistent throughout manuscript): NS p >0.05; * p ≤0.05; ** p ≤0.01; *** p ≤0.001; **** p ≤0.0001. Based on this analysis, we used a total microbial culture volume of 5 μl throughout the manuscript, unless otherwise noted.

26
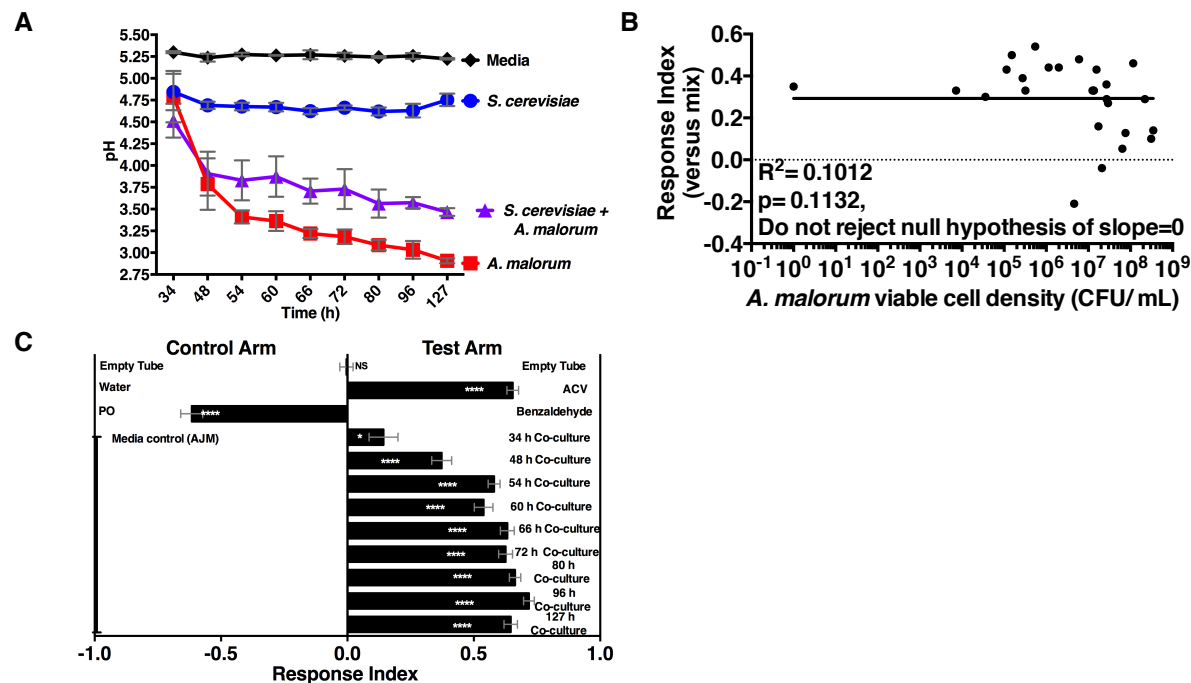
Figure 2-figure supplement 1. Properties of the co-culture and its relationship to *Drosophila* preference

(A) pH of experimental groups as a function of microbial growth time. Mean pH ± SEM of three experiments with one pooled replicate per experiment. **(B)** Relationship between *A. malorum* populations and *Drosophila* preference for the co-culture versus the separate-culture mixture. Each data point represents viable *A. malorum* populations in the co-culture along with the mean RI value toward the co-culture containing *A. malorum*. A semi-log standard curve with an unconstrained slope was generated and compared to a null model with slope=0. The data do not fit to an unconstrained slope better than to the null slope= 0 model (p=0.1132). **(C)** *Drosophila* attraction to the co-culture versus sterile media as a function of co-culture age (grown 34 h – 127 h). Mean RI ± SEM of three experiments with 16-18 total replicates. T-test against a hypothetical value of 0 was performed. NS p >0.05; * p ≤0.05; ** p ≤0.01; *** p ≤0.001; **** p ≤0.0001 Significance denoted beside or within bars of each experimental group. ACV = apple cider vinegar (25% in water); PO = paraffin oil.

27
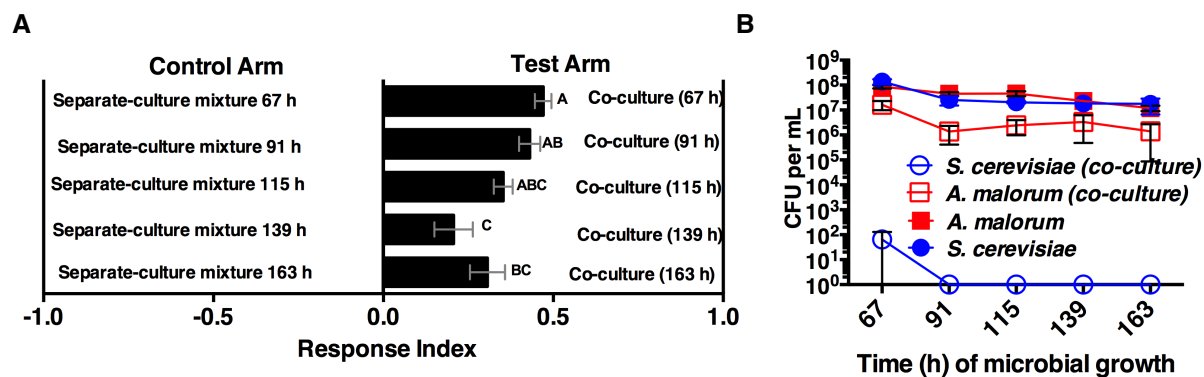
Figure 3-figure supplement 1. A) Attraction of wild-type *Drosophila* to different aged co-cultures (grown 67-163 h, *S. cerevisiae* and *A. malorum*). Mean ± SEM of 12-24 replicates per group (n=2-4 experiments). One-way ANOVA assessed significance between groups. A Tukey's multiple comparison test was used to assess significant differences between groups (p≤0.05), as indicated by unique letters. **B)** Corresponding viable counts at different times of microbial growth. Mean ± SEM of 2-3 replicates.

28
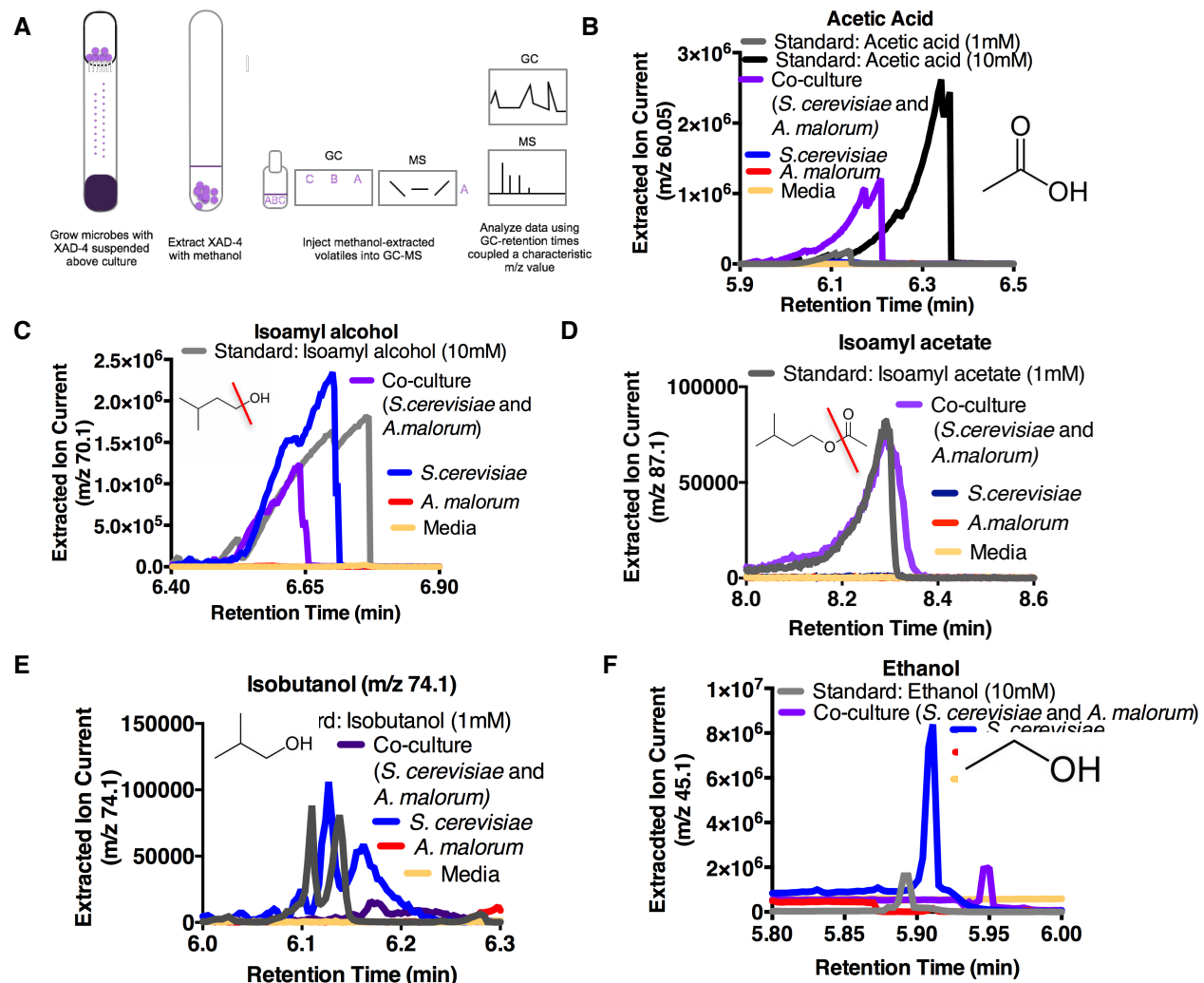
Table 1-figure supplement 1. Extracted ion chromatograms of the five metabolites detected by gas chromatography- mass spectrometry (GC-MS). **(A)** Schematic depicting the experimental setup **(B-F)** Representative extracted ion chromatograms from one replicate (out of three total) of one experiment (out of 3-4 total) of m/z values corresponding to major metabolites identified in the experimental conditions along with appropriate standards. Acetic acid **(B)**, isoamyl alcohol **(C)**, isoamyl acetate (**D**) isobutanol **(E)**, and ethanol **(F)** were identified as the five major metabolites in the co-culture (*S. cerevisiae* and *A. malorum*). Isoamyl alcohol **(C)**, ethanol **(E)**, and isobutanol **(F)** were identified as the major metabolites in *S. cerevisiae* grown alone. Extracted ion chromatograms were constructed using the m/z value in the title of each graph. For acetic acid and isobutanol, the m/z value used corresponds to the molecular weight of the molecule. For ethanol, the m/z used corresponds to the molecular weight minus one (hydrogen). For isoamyl alcochol, the m/z used corresponds to the loss of the hydroxyl group (depicted), which may have picked up a hydrogen and been lost as water. For isoamyl acetate, the m/z value corresponds to the molecule shown within the graph. In all cases, figures showing the complete mass spectra between the metabolite and standard are found in Table 1-figure supplement 2. Microorganisms were grown 72-96 hours.

29
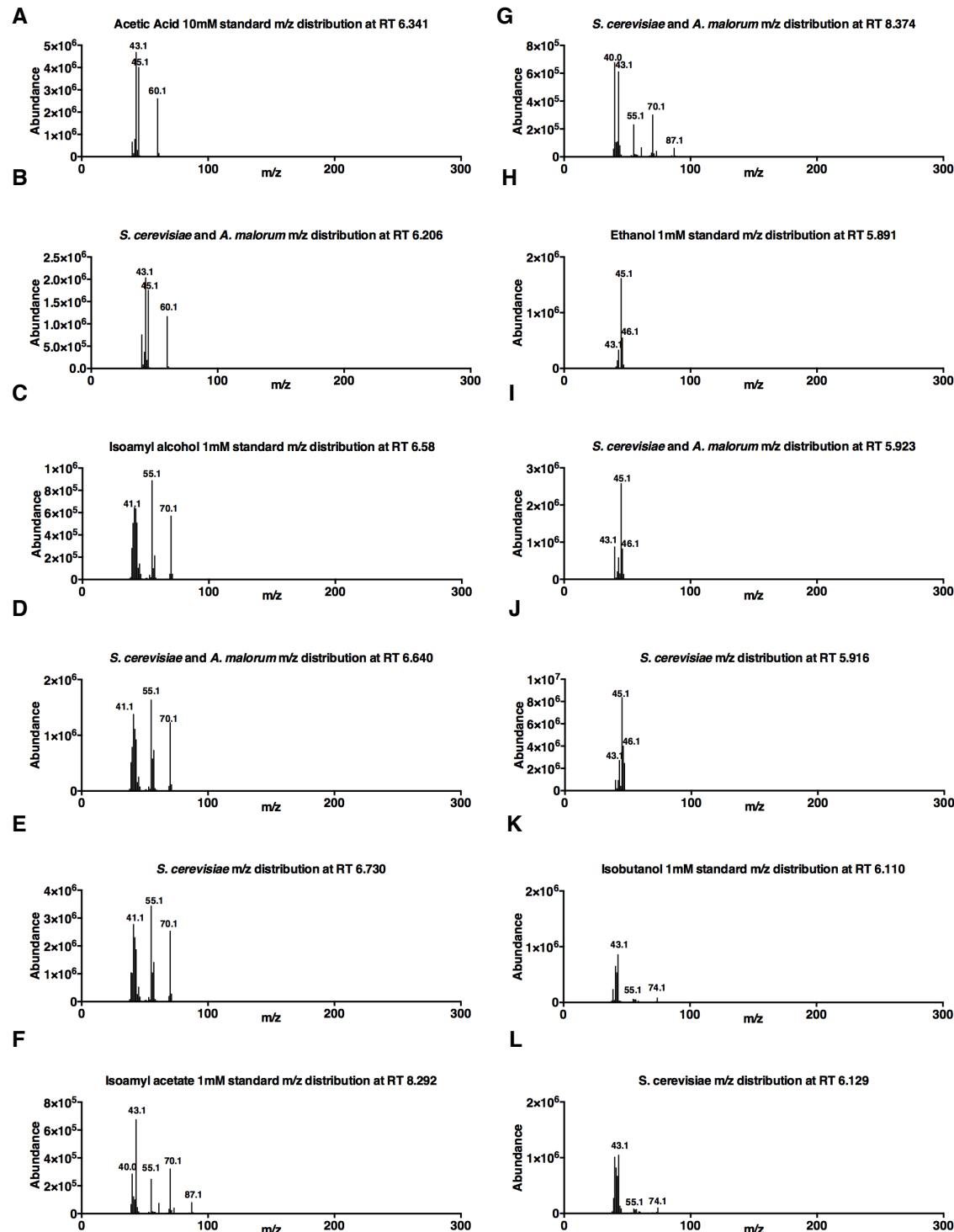
Table 1-figure supplement 2. Representative spectra of acetic acid (**A-B)**, isoamyl alcohol (**C-E)**, isoamyl acetate (**F-G)**, ethanol **(H-J)** and isobutanol **(K-L)** in standard and experimental samples**.** Standard concentrations are denoted on individual graphs. All mass spectra are one replicate (out of 3-4 experiments with three replicates per experiment).
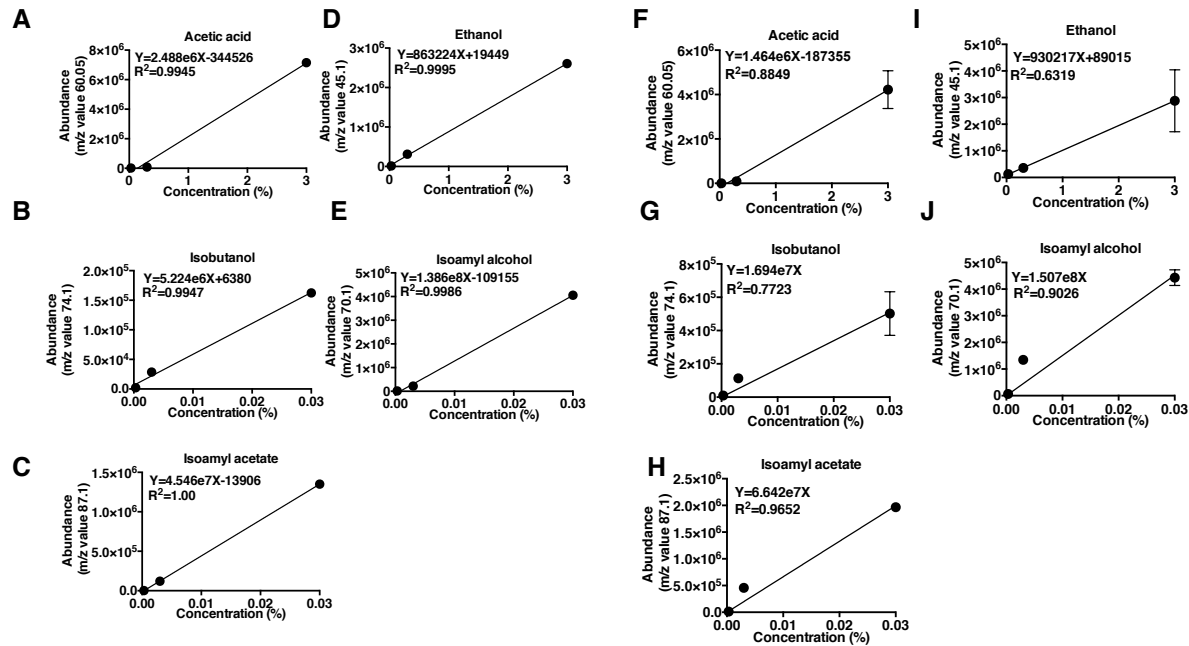
Table 1-figure supplement 3. Estimation of volatile quantity using GC-MS. Separate experiments are graphed in panels **(A-E)** and **(F-J)**. **(A-E)** Data points represent the value of a single replicate per concentration for each standard. The abundance of a single m/z value at a specific retention time was chosen for each standard. The values were fitted with a linear regression and the equation was used to estimate the concentration of the five metabolites in the experimental samples from the same experiment. **(F-J)** Data points represent the mean ± SEM of three replicates for a given concentration for each standard. The abundance of a single m/z value at a specific retention time was chosen for each standard. The values were fitted with a linear regression. The equation was used to estimate the concentration of the 5 metabolites in the experimental samples from the same experiment. When applicable an equation was calculated when the line was forced to go through X,Y=0,0; these equations were used to calculate the concentrations of isoamyl alcohol, isoamyl acetate, and isobutanol.

31
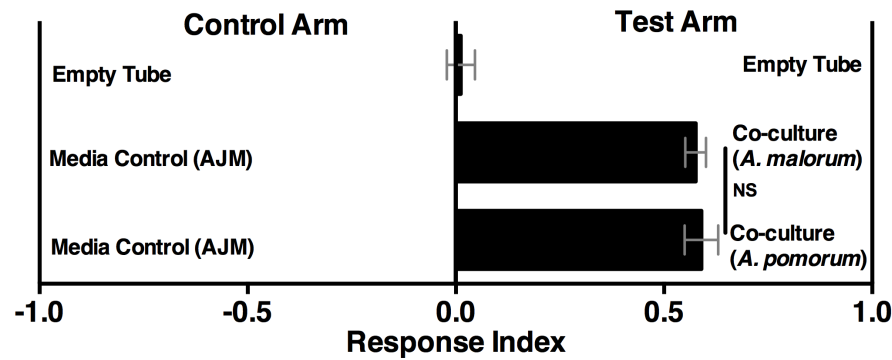
Figure 5-figure supplement 1. *Drosophila* behavior toward the co-culture using *A. malorum* or *A. pomorum*. *Drosophila* behavior toward co-cultures grown for 96 h using *A. malorum* or *A. pomorum* versus a media control (AJM = apple juice medium). Result of two experiments with six replicates each. Data points represent mean ± SEM. An unpaired two-tailed t-test assessed whether *Drosophila* behavior toward the co-cultures was different (NS p > 0.05).
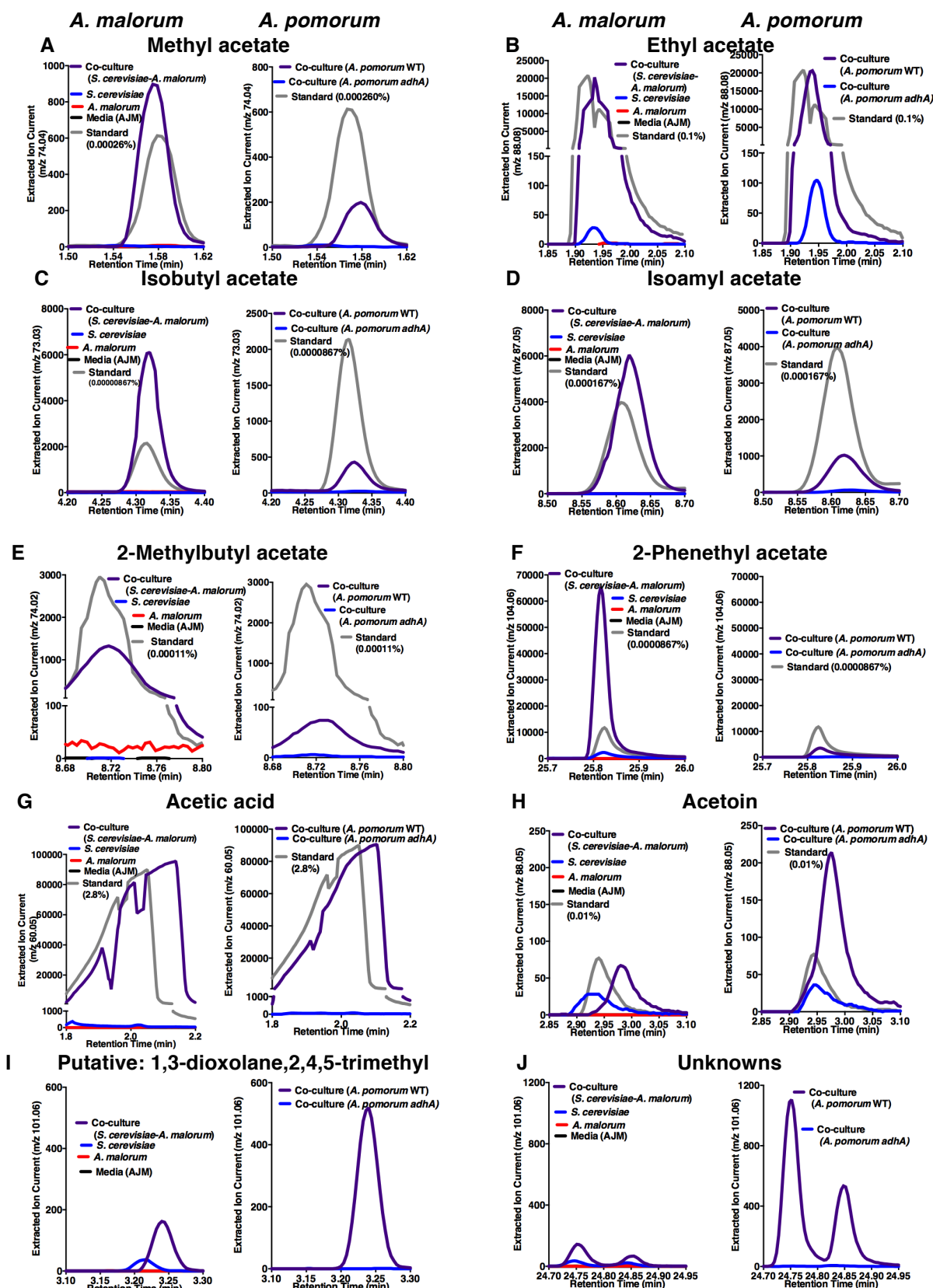
767 **Table 2-figure supplement 1.** Extracted ion chromatograms of differentially emitted or unique

768 metabolites in the co-culture according to solid phase microextraction gas chromatography-mass

769 spectrometry (SPME GC-MS). Specific metabolites are displayed above each panel. For each panel, the

770 left-most plot compares the co-culture containing *S. cerevisiae* and *A. malorum* to *S. cerevisiae* grown

771 alone, *A. malorum* grown alone, or media (AJM (apple juice medium)); the right-most plot compares the

772 co-culture containing *S. cerevisiae* and *A. pomorum* wild-type to the co-culture containing *S. cerevisiae*

773 and *A. pomorum adhA*, since *A. pomorum adhA* is required for *Drosophila* co-culture preference (Figure

774 5A). The two plots within the same panel contain the same standard. The y-axis for each plot is the ion

775 current for a m/z value that discriminates the metabolite of interest over a specific retention time window.

776 The following m/z values were chosen for each metabolite based on standards or, in the cases of putative

777 and unknown metabolites (**I** and **J**) were chosen from the experimental groups: **(A)** m/z 74.04 **(B)** m/z

778 88.08 **(C)** m/z 73.03 **(D)** 87.05 **(E)** 74.02 **(F)** 104.04 **(G)** 60.05 **(H)** 88.05 **(I)** 101.06 **(J)** 101.06. Each panel

779 is one representative replicate of 1 experiment (out of 3-5 total replicates in three experiments).

780

781

782

783

784

785

786

787

788

789

790

791

792

793

794

795

796

797

798

799

800

801

802

803

804

805

806

807

808

809

810

811

812

813

814

815

816

817

818

819

820

A

Isobutyl acetate

$Y = 4151*X - 0.1319$
$R^2 = 0.9828$

Normalized Peak Area vs Concentration (%, v/v)

F

Isobutyl acetate

$Y = 3252*X - 0.07251$
$R^2 = 0.9913$

B

2-Phenethyl acetate

$Y = 5129*X - 0.04011$
$R^2 = 0.9929$

G

2-Phenethyl acetate

$Y = 6972*X - 0.2013$
$R^2 = 0.9849$

C

Isoamyl acetate

$Y = 8158X$
$R^2 = 0.9607$

H

Isoamyl acetate

$R^2 = 0.9059$
$Y = 7800X$

D

2-Methylbutyl Acetate

$Y = 8995*X - 0.05041$
$R^2 = 0.9996$

I

2-Methylbutyl acetate

$Y = 8087*X - 0.1307$
$R^2 = 0.9981$

E

Methyl acetate

$Y = 75.22*X + 0.004457$
$R^2 = 0.9128$

Table 2-figure supplement 2. Normalized peak areas corresponding to metabolites in a defined metabolite mixture (from SPME GC-MS). A linear regression was calculated to quantify the metabolites in the co-culture. Each concentration is from one replicate. **A-E** and **F-I** are two separate experiments. Linear regression was used to estimate the concentration of the metabolites in the co-culture containing *S. cerevisiae* and *A. malorum* (Table 2) and to complement the co-culture containing *A. pomorum adhA* (Figure 5A).

35

821

822

823

824

825

826

827
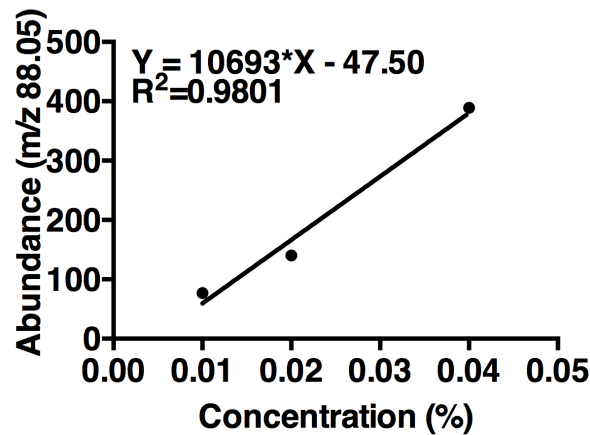
828   **Figure 6-figure supplement 1.** Acetoin linear regression. The curve is based on maximum m/z values

829   (88.05) of three concentrations of acetoin. One replicate per concentration (n=1 experiment). The linear

830   regression was used to estimate acetoin concentrations in the tri-culture and the co-culture (Figure 6B).

831

832

833

834

835

836

837

838

839

840

841

842

843

844

845

846

847

848
849
850
851
852
853
854
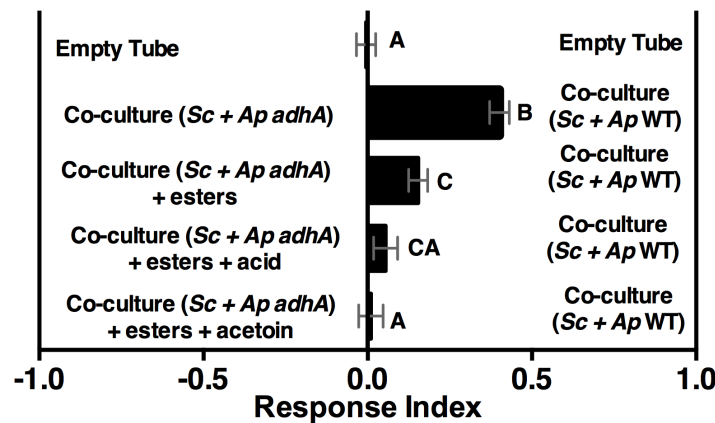
855 **Figure 6-figure supplement 2.** Role of esters alone or esters with acetoin in complementing co-culture

856 with *A. pomomrum adhA*. Mean +/- SEM of three experiments with 16-18 total replicates. A one-way

857 ANOVA assessed whether groups were different. A Tukey's multiple comparison test was used to assess

858 significant differences between groups (p≤0.05), as indicated by unique letters. Esters include ethyl

859 acetate, isoamyl acetate, 2-phenethyl acetate, isobutyl acetate, 2-methylbutyl acetate, and methyl

860 acetate. Esters added are based on physiological amounts in co-cultures and are calculated in Table 2

861 and Table 2-figure supplement 2). Acetoin is added in a similar amount as the tri-culture (Figure 6A,

862 0.3%). *Sc = S. cerevisiae, Ap = A. pomorum*.

863
864
865
866
867
868
869
870
871
872
873
874

37
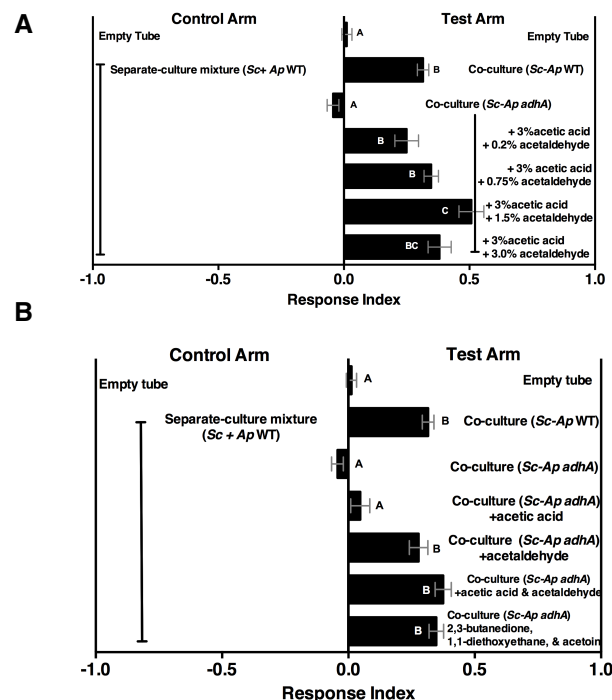
Figure 6-figure supplement 3. Acetaldehyde metabolic derivatives can complement the co-culture containing *A. pomorum adhA*, although their physiological concentrations are unknown. **(A)** Dose response of acetaldehyde was given to the co-culture containing *A. pomorum adhA* (along with a constant dose of 3.0% acetic acid). Metabolite additions were added to the culture in the noted percentages, allowed to sit 35 minutes at room temperature, mixed 1:1 in water, and assessed for *Drosophila* attractivess. Mean ± SEM of 1-7 experiments with 12-42 total replicates per group. The experimental groups from one experiment were run in two separate groups during the day. Differences between groups were tested by one-way ANOVA. A Tukey's multiple comparison test was used to assess significant differences between groups (p≤0.05), as indicated by unique letters. **(B)** Role of acetic acid, acetaldehyde, or specified acetaldehyde metabolic derivatives in complementing the co-culture containing *A. pomorum adhA*. Acetic acid (3.0%) and acetaldehyde (0.75%) were added and allowed to sit at room temperature for 35 minutes, mixed 1:1 in water, and *Drosophila* attraction was assayed. 2,3-butanedione (0.15%), 1,1-diethoxyethane (0.01%), and acetoin (0.15%) were added to the culture, mixed 1:1 with water, and *Drosophila* behavior was assayed. Mean ± SEM of 2-7 experiments with 5-6 replicates per experiment. Differences between groups were tested by one-way ANOVA. A Tukey's multiple comparison test was used to assess significant differences between groups (p≤0.05), as indicated by unique letters. *Sc = S. cerevisiae, Ap = A. pomorum*.

38
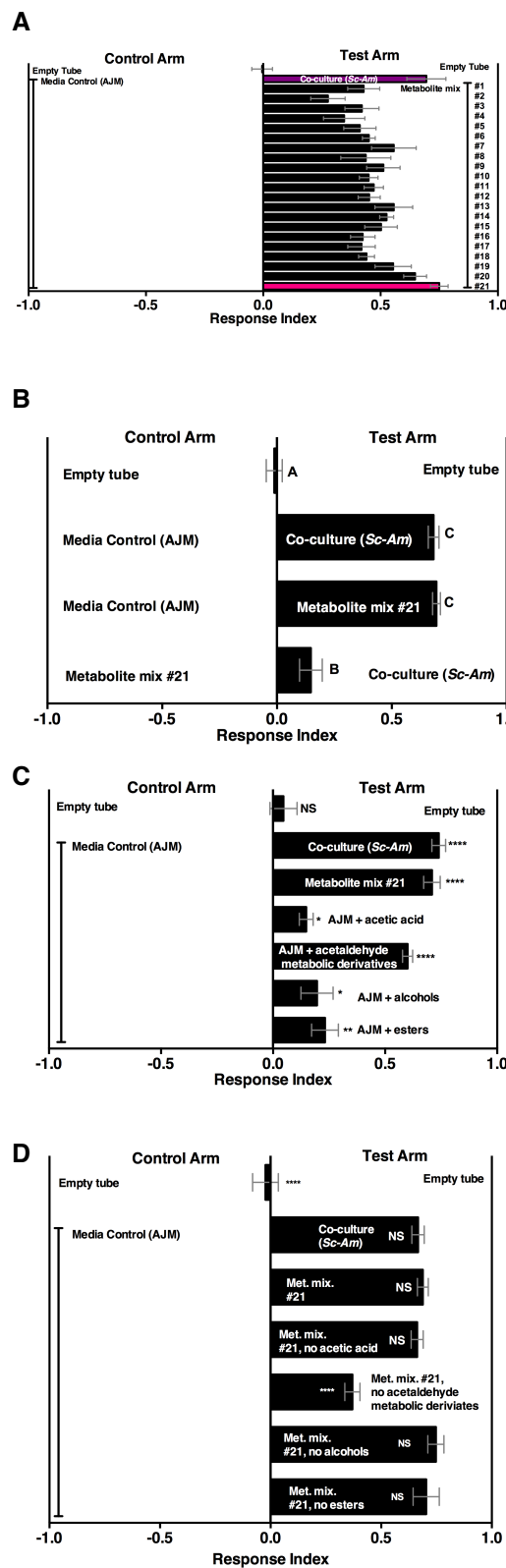
Figure 6-figure supplement 4. *Drosophila* behavior toward metabolite mixtures and their component parts **(A)** *Drosophila* behavior toward 21 metabolite mixtures versus AJM (50% in water). Methods Table 4 contains the concentrations of all mixtures (in 50% AJM). The co-culture (*S. cerevisiae* and *A. malorum*, purple bar) was grown for 96 h. The pink bar is metabolite mixture #21 and most closely resembled the co-culture. Mean ± SEM of 4-6 replicates per experimental group. Groups were run over five different days. **(B)** Relative *Drosophila* attraction to a co-culture grown for 96 h and metabolite mixture #21. Mean ± SEM of three experiments with 17-18 replicates per group. One-way ANOVA assessed whether the groups were different. A Tukey's multiple comparison test was used to assess significant differences between groups (p≤0.05), as indicated by unique letters. **(C)** The sufficiency of individual groupings within metabolite mixture #21 to attract *Drosophila*. The individual grouping are as follows: acetaldaldehyde metabolic derivatives (1,1-diethoxyethane; acetoin; 2,3-butanedione); alcohols (ethanol; isobutanol; isoamyl alcohol; 2-methyl, 1-butanol; benzeneethanol); esters (isoamyl acetate; ethyl acetate; isobutyl acetate; 2-phenethyl acetate; butyl acetate; 2-methylbutyl acetate; methyl acetate; phenethyl benzoate; propyl acetate; ethyl isobutyrate; ethyl hexanoate; isovaleric acid; butyl ester; ethyl octanoate; ethyl decanoate; ethyl laurate); and acetic acid (acetic acid). Concentrations are in Methods Table 4. Mean ± SEM of six replicates of one experiment (except the acetaldehyde metabolic derivative group which is 12 replicates from 2 experiments). A t-test against a hypothetical value of 0 was performed. p >0.05; * p ≤0.05; ** p ≤0.01; *** p ≤0.001; **** p ≤0.0001 **(D)** The same groups used in **C** were used and removed from metabolite mix #21. The difference between the co-culture (*Sc-Am*) and each group was assessed by one-way ANOVA. A Tukey's multiple comparison test was used to assess significant differences between groups (p≤0.05), as indicated by unique letters. Mean ± SEM of six replicates of one experiment are shown.

39
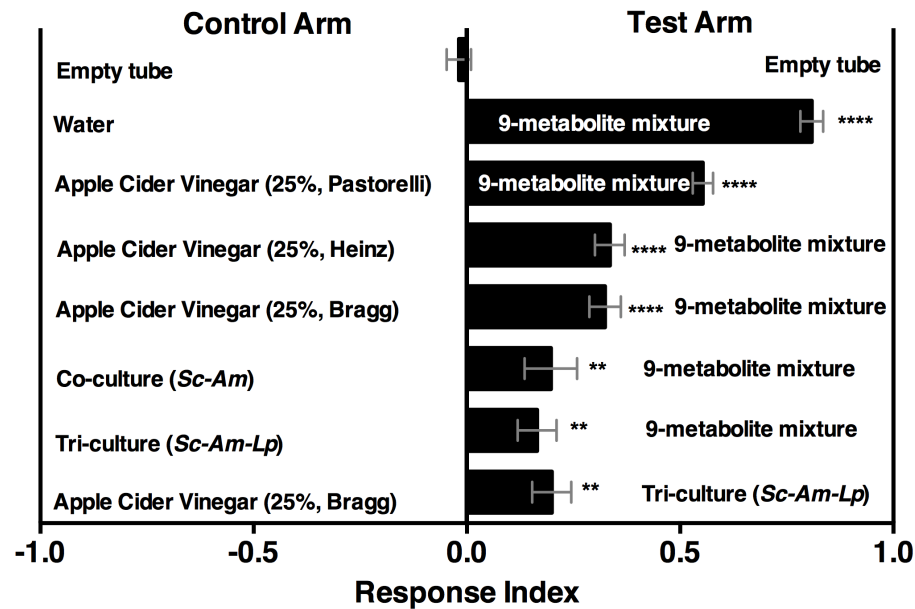
Figure 6-figure supplement 5. *Drosophila* behavior toward water amended with 9 metabolites (9-metabolite mixture) versus 3 different apple cider vinegars (ACV), a co-culture (*Sc-Am = S. cerevisiae* and *A. malorum*), or tri-culture (*Sc-Am-Lp = S. cerevisiae, A. malorum*, *L. plantarum* cs). Cultures were grown for 72 h and mixed 1:1 with water, as in all other experiments. Data points represent the Mean ± SEM of two experiments with twelve total replicates. A one-way ANOVA assessed whether each group was different from the mock condition (empty tube versus empty tube). $p > 0.05$; * $p \leq 0.05$; ** $p \leq 0.01$; *** $p \leq 0.001$; **** $p \leq 0.0001$. The acetoin concentration was similar to that calculated from the tri-culture (Figure 6A, 0.3%). The concentrations of all 9 metabolites can be found in the materials and methods.

40

956 **MATERIALS AND METHODS**

957 *Fly maintenance*

958 Fly stocks, genotypes, and sources are listed in Methods Table 1. *Drosophila melanogaster* was reared at

959 25°C on a 12h:12h light: dark cycle on autoclaved food (5% yeast, 10% dextrose, 7% cornmeal, 0.6%

960 propionic acid, 0.7% agar).

961

962 *Microbial strains*

963 Microorganisms used in this study are listed and described in table S1. Microorganisms were streaked

964 onto yeast-peptone dextrose (YPD; 1% yeast extract (Becton Dickinson, and Company, Franklin Lakes,

965 NJ, USA), 2% peptone (Becton Dickinson, and Company, Franklin Lakes, NJ, USA), and 2% dextrose

966 (Avantor Performance Materials, Center Valley, PA, USA)) or Man, de Rosa, Sharpe (MRS, Fisher

967 Scientific, Waltham, MA, USA) plates from a freezer stock.

968

969 *T-maze olfactory attraction assays*

970 The T-maze apparatus was a kind gift of the Carlson Laboratory. Flies were wet-starved for 15-26 hours

971 prior to T-maze olfactory experiments by placing flies into vials containing Kimwipes (Kimberly Clark,

972 Dallas, TX, USA) soaked with 2 mL of milliQ water. Flies were collected within 4 days (<65 flies per vial)

973 of emergence and matured on autoclaved food. Flies between 3 and 10 days-old were used in

974 experiments.

975

976 Single microbial colonies were picked from rich media (MRS and YPD) plates and grown overnight.

977 Cultures were washed 1X in PBS, diluted 100-fold, and 10μl was aliquoted into 3mL of apple juice media

978 (AJM, apple juice (Martinelli's Gold Medal, Watsonville, CA, USA), pH adjusted to 5.3 with 5M NaOH, with

979 0.5% yeast extract). Media was filtered with a 0.22 μM-size pore attached to a 250-mL polystyrene bottle

980 (Corning, NY, USA). For co-culture experiments, 1e3-1e5 CFU of each microorganism was placed

981 simultaneously into AJM. Microorganisms were grown in 14-mL round bottom polypropylene tubes

982 (Corning Science, Tamaulipas, Mexico) at 28°C, 200rpm for the time noted in individual experiments. The

41

983   microbial culture was diluted 1:1 with sterile milliQ water (0.22 μM filter (Millipore, Billerica, MA, USA))

984   and placed directly onto autoclaved 10 mM round Whatman filter paper (GE Healthcare Life Science,

985   Pittsburgh, PA, USA) placed near the bottom of 15mL CentriStar centrifuge tubes (Corning, NY). A total

986   volume of 10 μl was used for all experiments.

987

988   Tubes containing microorganisms and *Drosophila* were placed into the behavioral room (20-25°C, 50-

989   70% humidity maintained by a humidifier (Sunbeam Tower Humidifier, Boca Raton, FL, USA) and

990   equilibrated for 10 minutes prior to the beginning of the experiment. Flies (~40-130) were knocked into the

991   T-maze apparatus, rested for ~1 min, and then allowed to choose from the test and control arms for 2 min

992   in the dark. The test arm was alternated from one side of the apparatus to the other every experimental

993   replicate. A Response Index (RI) was computed to analyze preference for the test arm (flies in test arm-

994   flies in control arm)/(total flies).

995

996   *Chemicals*

997   Chemicals can be found in Methods table 2**.**

998

999   *Microbial populations and pH*

1000   Selective plates were used to distinguish *S. cerevisiae* from *A. malorum*. MRS containing 50 μg/mL

1001   cycloheximide selected for *A. malorum* while MRS containing 10 μg/mL chloramphenicol and 20 μg/mL

1002   tetracycline selected for *S. cerevisiae*. pH of filtered cultures (0.22 μM) was measured using a Beckman

1003   Coulter pH meter (Model Phi510, Fullerton, CA, USA).

1004

1005   *Gas chromatography- Mass spectrometry*

1006   Microbial samples were grown in AJM for a specified amount of time in 14-mL round bottom tubes fitted

1007   with an autoclaved tissue strainer (250 μM nylon mesh (Thermo Scientific Pierce, Grand Island, NY)

1008   holding between 0.03 and 0.05 grams of autoclaved Amberlite XAD-4 resin (Sigma-Aldrich, St Louis, MO,

1009   USA) prewashed in water and methanol. After microbial growth, XAD-4 from two cultures was dumped

1010   into an autoclaved glass vial. XAD-4 was swirled with 900μl methanol for 30 seconds. 500-750μl of

1011   methanol was removed for GC-MS analysis. Quantification for table S2 was derived from beads

1012   suspended above the cultures from 84-96 h of growth. Quantification for Fig. 2D was derived from beads

1013   suspended above the culture every 12 h; time points on the graph refer to the end point of the 12-h span

1014   (e.g. 84 h corresponds to beads suspended from 72-84 h of growth).

1015

1016   Samples (5 μl of methanol-extracted samples) were injected into the GC-MS (Agilent 7890A/5975C) at

1017   250 °C using helium as the carrier gas at a flow rate of 1.1 mL per minute (column head pressure 13 psi).

1018   The following chromatography temperature program was used for experiments to initially identify

1019   metabolites in the co-culture and individually grown microorganisms: 40°C for 3 min ramped at 1.7°C per

1020   minute to 200 °C (held for 3 min) then to 220°C at 3 °C per min and held for a further 5 min. The total run

1021   time was 111.78 min. For experiments focused on the five major metabolites, a shorter program was used

1022   that maintained the same first 10 min of the previous method (all 5 volatiles eluted within 9 min). The

1023   chromatography temperature program was 40°C for 3 min, ramped at 1.7°C per min to 46.8°C and held

1024   for 3 min, then ramped at 60°C per min until 220°C and held for 5 min. The total run time was 17.9 min.

1025

1026   The mass spectrometer was run in electron-impact (EI) mode at 70 eV. The temperatures of the transfer

1027   line, quadrupole, and ionization source were 220°C, 180°C, and 230°C respectively. The ionization was

1028   off during the first 4 min to avoid solvent overloading with a source temperature of 230°C. Mass spectra

1029   were recorded in the range of 35-300 m/z. Full scan mode was used at a scan rate of 6 scans/sec. The

1030   electron multiplier voltage was set in the relative mode to autotune procedure.

1031

1032   In the initial experiments peaks were manually picked using Agilent Chemstation Software. Volatiles

1033   associated with peaks were searched against the National Institute of Standards (NIST) 11 database.

1034   Subsequent experiments focused on the 5 major volatiles identified in the initial experiments by

1035   performing extracted ion chromatograms using an ion that successfully identified a standard at a specific

1036   retention time. Quantification was performed by tabulating the maximum abundance of the ion at a

1037 characteristic retention time and using a linear regression equation from a dose-response of the

1038 standards (fig. S6).

1039

1040 *Headspace solid phase microextraction (SPME) Gas chromatography- Mass spectrometry*

1041 A Waters GCT Premier gas chromatography time of flight mass spectrometer (Milford, MA) with a DB-

1042 5MS column (30m x 0.25 mm ID x 0.25 µm film thickness; Agilent) was used. Live cultures were

1043 transferred to autoclaved glass vials (20 mL, 23 X 75 mm, Supelco, Bellefonte, PA, USA) with screw caps

1044 (18mm, 35 Shore A, Supelco, Bellefonte, PA, USA) after growing for 72 h.

1045

1046 The glass vials containing live microbial cultures were analyzed via a 50/30µm

1047 carboxen/divinylbenzene/polydimethylsiloxane Stableflex solid-phase micro-extraction (SPME) fiber. The

1048 extraction methodology was based on previous studies using SPME to extract volatiles form vinegars (65,

1049 66). The syringe was inserted through the membrane of the caps and sampled the volatiles for 30 min at

1050 45°C; subsequently, metabolites were desorbed for 30 sec at 240C and baked for an additional 4.5 min in

1051 the injection port. The gas chromatograph was fitted with a microchannel plate (MCP) detector. The

1052 temperature program of the column was as follows: 40°C for 5 min, 2°C a min for 17.5 min followed by

1053 25°C a min for 10 min. A final hold time of 5 min at 325°C was used. The carrier gas was helium. A split

1054 ratio of 250 was used based on better peak resolution. An internal standard of cineole (Sigma-Aldrich, St.

1055 Louis, MO, USA) was run with each sample and used to compute relative abundances. The mass

1056 detector was in the range of 40 to 650 m/z.

1057

1058 To analyze the data, MassLynx software was used. The response threshold was set to an absolute area

1059 of 10.00. The software automatically picked out peaks and computed peak areas. To obtain a relative

1060 quantification, peaks were compared across samples and normalized to the internal standard. Peaks

1061 were first searched against the NIST5 database to identify potential hits. Most potential metabolites were

1062 confirmed by a standard mixture in 50% AJM. The standard mixtures are in Methods Table 3**.**

1063

1064   *Chemical complementation of co-culture containing A. pomorum PQQ-ADH-I*

1065   A co-culture containing *S. cerevisiae* and *A. pomorum* WT or *A. pomorum PQQ-ADH-I* was grown for 72

1066   h before use in the T-maze. For the physiological concentrations of acetate-derived metabolites,

1067   concentrations were added as in table S3 and then mixed 1:1 with water prior to behavioral analysis. For

1068   the acetaldehyde metabolic derivatives chemical complementation group, a 1:1 mixture of the mutant co-

1069   culture: water was supplemented with 1,1-diethoxyethane, 2,3-butanedione, and acetoin at final

1070   concentrations of 0.01%, 0.15% and 0.15%, respectively and used immediately in the T-maze. Acetic

1071   acid and/or acetaldehyde were added to the culture, allowed to sit at RT for 35 min, mixed 1:1 with water

1072   and then placed into the T-maze vials.

1073

1074   Standard curves were used to calculate the concentrations of individual metabolites (fig. S10). The

1075   standard curves were generated on 2 separate experiments in which 3 concentrations of each standard

1076   was used. The concentrations of the metabolites were independently calculated from the standard curve

1077   equations generated on the two separate days. Estimated concentrations from each standard curve

1078   equation were averaged (table S3). The experimental data is based on the peak areas of the

1079   *S.cerevisiae-A. malorum* co-culture.

1080

1081   *Ester, acid, and acetaldehyde metabolic derivative mixture*

1082   The 9-metabolite mixture contains 1.5% acetic acid, 0.0003% isoamyl acetate, 0.0003% 2-phenethyl

1083   acetate, 0.01% ethyl acetate, 0.002% ethyl lactate, 0.3% 1,1-diethoxyethane, 0.3% 2,3-butanediol, 0.3%

1084   2,3-butanedione, and 0.3% acetoin in filtered milliQ water.

1085

1086   Drosophila *survival in the presence of ethanol and acetic acid*

1087   Adult male flies (0-3 d-old) were collected and matured for 1 day on fly food. Flies were then placed into

1088   vials containing kimwipes with 5 mL of either Shields & Sang Insect Medium (Sigma, St. Louis, MO;

1089   positive control), MilliQ water (negative control), or MilliQ water with ethanol (9.4%), acetic acid (3.42%),

1090   or ethanol and acetic acid (1.4 and 2.8% respectively). Survival was assessed every 12 h for 7 d. For

1091   each condition 5 mL was given at 0 and 12 h and every 24 h thereafter. Experimental replicates were

1092   considered separate vials (5-6 per group). Each replicate contained 8-31 flies.

1093

1094   *Egg-laying preference assay*

1095   Egg-preference assay was adapted from Joseph *et al* 2009 (67). Microbial cultures grown for 96 h were

1096   heated to 65°C for 10 min, mixed 1:1 with 1.6% agarose and poured into a 35 mm petri dish separated in

1097   two by a straight-edge razor blade. Flies were starved for ~18 h prior to the experiment. The 35 mm petri

1098   dish was placed within clear flat top boxes with dimensions 2 5/16" X 2 5/16" X 5 1/16" (TAP plastics, San

1099   Leandro, CA, USA). The test and control sides were alternated for each replicate. *Drosophila* aged 4-10

1100   days (n=50-100) was allowed to lay eggs for 8 h. After the assay, the number of eggs on deposited on

1101   each choice was tabulated and an egg-laying index was computed analogously to the olfactory response

1102   index.

1103

1104   *Data analysis*

1105   Data analysis was performed in Prismv6.0b. Specific statistical tests are noted for individual experiments.

1106

Methods Table 1. *Drosophila melanogaster* stocks used in experiments

Notation	Gene Mutant	Genotype	Source
CS	NA	w+-Canton-S	John Carlson Laboratory
Or83b	*Or83b*	w-Canton-S;;orco2	John Carlson Laboratory
Ir64a	*Ir64a*	w[1118]; Mi{ET1}Ir64a[MB05283]	Bloomington Stock Center
Ir75a	*Ir75a*	y[1] w[67c23]; Mi{ET1}Ir75a[MB00253]	Bloomington Stock Center
W-CS	NA	w-Canton-S	John Carlson Laboratory
Balancer	NA	w-CS;Sp/Cyo;Dr/TM3B	John Carlson Laboratory
Ir25a	*Ir25a*	w^{1118}; Mi{ET1}Ir25a^{MB09568}	Bloomington Stock Center
Ir8a	*Ir8a*	Ir8a^{1}; Bl^{1} L^{2}/CyO	Bloomington Stock Center
Ir76b	*Ir76b*	y1 w67c23; Mi{ET1}Ir76bMB00216	Bloomington Stock Center
Or42b	*Or42b*	w; or42b/or42b; +/+	John Carlson Laboratory
Or35a	*Or35a*	W; or35a/or35a; +/+	John Carlson Laboratory

Chemical	Company	Location
Paraffin Oil	EMD chemicals	Gibbstown, NJ, USA
Apple Cider Vinegar	Heinz	Pittsburgh, PA, USA
Apple Cider Vinegar (unpasteurized)	Bragg (Fig. 3C only)	Santa Barbara, CA, USA
Apple Cider Vinegar	Pastorelli (Fig. 3C only)	Chicago, IL, USA
Benzaldehyde	Sigma Aldrich	St. Louis, MO, USA
2-Methyl-1-Propanol (Isobutanol)	Sigma Aldrich	St. Louis, MO, USA
Isopentyl Acetate (Isoamyl Acetate)	Sigma Aldrich	St. Louis, MO, USA

Isoamyl Alcohol	Avantor Performance Materials	Center Valley, PA, USA
Acetic Acid, glacial	Avantor Performance Materials	Center Valley, PA, USA
Methanol	Avantor Performance Materials	Center Valley, PA, USA
Ethanol, 200 proof	Decon Laboratories	King of Prussia, PA, USA
Acetal (1,1, diethoxyethane)	Fisher	Pittsburgh, PA, USA
Acetaldehyde	Acros Organics	Grand Island, NY
Ethyl acetate	Sigma Aldrich	St. Louis, MO, USA
1-pentanol	Sigma Aldrich	St. Louis, MO, USA
Benzeneethanol (2-phenylethanol)	Fisher	Pittsburgh, PA, USA
Isobutyl acetate	Sigma Aldrich	St. Louis, MO, USA
2-phenethyl acetate	Sigma Aldrich	St. Louis, MO, USA
Butyl acetate	Sigma Aldrich	St. Louis, MO, USA
2-methylbutyl acetate	TCI	Tokyo, Japan
Methyl acetate	Sigma Aldrich	St. Louis, MO, USA
Acetoin acetate	Sigma Aldrich	St. Louis, MO, USA
Phenethyl formate	Sigma Aldrich	St. Louis, MO, USA
Phenethyl benzoate	Sigma Aldrich	St. Louis, MO, USA
acetoin	Sigma Aldrich	St. Louis, MO, USA
2,3-butanedione	Sigma Aldrich	St. Louis, MO, USA
2-methyl-1-butanol	Sigma Aldrich	St. Louis, MO, USA
Ethyl lactate	Sigma Aldrich	St. Louis, MO, USA
1-hexanol	Sigma Aldrich	St. Louis, MO, USA
Phenylacetic acid	Sigma Aldrich	St. Louis, MO, USA
2,3-butanediol	Sigma Aldrich	St. Louis, MO, USA
Ethyl octanoate	Sigma Aldrich	St. Louis, MO, USA
Ethyl decanoate	Sigma Aldrich	St. Louis, MO, USA

Ethyl hexanoate	Sigma Aldrich	St. Louis, MO, USA
Ethyl laurate	Sigma Aldrich	St. Louis, MO, USA
Ethyl isobutyrate	Sigma Aldrich	St. Louis, MO, USA
phenylacetaldehyde	Sigma Aldrich	St. Louis, MO, USA
Butyl isovalerate	TCI	Tokyo, Japan
Propyl acetate	Sigma Aldrich	St. Louis, MO, USA

1107

Methods Table 3. Metabolite mixture concentrations used for identification and quantification in SPME GC-MS

Metabolite	Met mix 1	Met mix 2	Met mix 3
Ethanol	0.20%	1.00%	2.00%
Isobutanol	0.0040%	0.0010%	0.000250%
Acetic acid	2.80%	4.320%	1.920%
Isoamyl alcohol	0.00150%	0.0030%	0.0060%
Isoamyl acetate (1-butanol, 3-methyl acetate)	0.00050%	0.000167%	0.00150%
Acetal (1,1-Diethoxyethane)	0.020%	0.10%	0.0050%
Acetaldehyde	0.020%	NONE	0.0040%
Ethyl acetate	0.0050%	0.10%	0.020%
Benzeneethanol (2-phenylethanol)	0.00360%	0.00040%	0.00120%
Isobutyl acetate	0.000260%	0.0000867%	0.0000289%
2-Phenethyl acetate	0.000260%	0.0000867%	0.0000289%
2-Methylbutyl acetate (1- butanol 2-methyl acetate)	0.0010%	0.00033%	0.00011%
Methyl acetate	0.0000867%	0.0000289%	0.000260%
2-Methyl, 1-butanol	0.00030%	0.00150%	0.00450%
2,3-Butanedione	NONE	0.010%	0.0020%
Acetoin (1g/10mL h20, 10%)	0.01%	0.020%	0.040%

49

2,3-Butanediol	NONE	0.10%	0.020%
Propyl acetate	0.000020%	0.0000020%	NONE*

1108   *1/2 experiments had a concentration of 0.0000

1109   **Methods Table 4.** Composition of metabolite mixtures 1-21 used in figure S14

Volatile	Metabolite mixture																				
	1	2	3	4	5	6	7	8	9	10	11	12	13	14	15	16	17	18	19	20	21
Ethanol	0.5700	0.5700	0.5700	0.5700	0.5700	0.5700	0.5700	0.5700	0.5700	0.5700	0.2850	0.2850	0.2850	0.2850	0.2850	0.2850	0.5700	0.5700	0.5700	0.5700	0.5700
Isobutanol	0.0007	0.0007	0.0007	0.0007	0.0007	0.0007	0.0007	0.0007	0.0007	0.0007	0.0004	0.0004	0.0004	0.0004	None	0.0004	0.0005	0.0007	0.0007	0.0007	0.0007
Acetic acid	1.4400	1.4400	1.4400	1.4400	1.4400	1.4400	1.4400	1.4400	1.4400	1.4400	1.4400	1.4400	1.4400	1.4400	1.4400	1.4400	1.4400	1.4400	1.4400	1.4400	1.4400
Isoamyl alcohol	0.0010	0.0010	0.0010	0.0010	0.0010	0.0010	0.0010	0.0010	0.0010	0.0005	0.0005	0.0005	0.0005	0.0005	0.0002	0.0005	0.0005	0.0010	0.0010	0.0010	0.0010
Isoamyl acetate	0.0007	0.0007	0.0007	0.0007	0.0007	0.0007	0.0007	0.0007	0.0010	0.0007	0.0005	0.0007	0.0007	0.0007	0.0007	0.0007	0.0007	0.0007	0.0007	0.0007	0.0007
1,1-diethoxyethane	0.0100	0.0300	0.0100	None	0.0033	0.0100	0.0100	0.0010	0.0200	0.0100	0.0050	0.0100	0.0300	0.0500	0.0500	0.0030	0.0030	0.0030	0.0100	0.0100	0.0100
acetaldehyde	0.0100	0.0100	0.0100	0.0100	0.0100	0.0100	0.0100	0.0010	0.0100	0.0100	0.0050	0.0050	0.0050	0.0050	0.0025	0.0025	None	None	None	None	None
ethyl acetate	0.0010	0.0010	0.0010	0.0010	0.0010	0.0010	0.0010	0.0010	0.0020	0.0010	0.0005	0.0010	0.0010	0.0010	0.0010	0.0010	0.0010	0.0007	0.0007	0.0007	0.0007
1-pentanol	0.0010	0.0010	0.0010	0.0010	0.0010	0.0010	0.0010	0.0010	0.0010	0.0005	0.0003	0.0005	0.0005	0.0005	0.0002	None	None	None	None	None	None
benzeneethanol	0.0010	0.0010	0.0010	0.0010	0.0010	0.0010	0.0010	0.0010	0.0010	0.0005	0.0003	0.0005	0.0005	0.0005	0.0002	0.0005	0.0005	0.0005	0.0005	0.0005	0.0005
isobutyl acetate	0.0010	0.0010	0.0010	0.0010	0.0010	0.0010	0.0010	0.0010	0.0010	0.0010	0.0005	0.0010	0.0010	0.0010	0.0010	0.0010	0.0010	0.0007	0.0007	0.0007	0.0007
2-phenethyl acetate	0.0010	0.0010	0.0010	0.0010	0.0010	0.0010	None	0.0010	None	None	0.0005	0.0010	0.0010	0.0010	0.0010	0.0010	0.0010	0.0007	0.0007	0.0007	0.0007
butyl acetate	0.0010	0.0010	0.0010	0.0010	0.0010	0.0010	None	0.0010	None	None	0.0005	0.0010	0.0010	0.0010	0.0010	0.0010	0.0010	0.0007	0.0007	0.0007	0.0007
2-methylbutyl acetate	0.0010	0.0010	0.0010	0.0010	0.0010	0.0010	0.0010	0.0010	0.0020	0.0010	0.0005	0.0010	0.0010	0.0010	0.0010	0.0010	0.0010	0.0007	0.0007	0.0007	0.0007
methyl acetate	0.0010	0.0010	0.0010	0.0010	0.0010	0.0010	0.0010	0.0010	0.0010	0.0010	0.0005	0.0010	0.0010	0.0010	0.0010	0.0010	0.0010	0.0007	0.0007	0.0007	0.0007
2-acetoxy-3-butanone	None	None	0.0010	0.0010	0.0010	0.0010	None	0.0010	None	None	0.0005	0.0010	0.0010	0.0010	0.0010	None	None	None	None	None	None
phenethyl formate	None	None	0.0010	0.0010	0.0010	0.0010	None	0.0010	None	None	0.0005	None	None	None	None	None	None	None	None	None	None
phenethyl benzoate	None	None	0.0010	0.0010	0.0010	0.0010	0.0010	0.0010	0.0010	0.0010	0.0005	0.0010	0.0010	0.0010	0.0002	0.0010	0.0010	0.0007	0.0007	0.0007	0.0007
2-methy, 1-butanol	None	None	None	None	None	0.0010	0.0010	0.0010	0.0010	0.0005	0.0005	0.0005	0.0005	0.0005	0.0005	0.0005	0.0005	0.0005	0.0005	0.0005	0.0005
2,3butanedione	None	None	None	None	None	0.001	0.0010	0.0010	0.0010	0.0010	0.0005	0.0010	0.0030	0.0050	0.0050	0.0030	0.0030	0.0030	0.0100	0.0500	0.1500
acetion (10% m/v, H$_2$0)	None	None	None	None	None	0.001	0.001	0.0010	0.0020	0.0010	0.0005	0.0010	0.0030	0.0050	0.0050	0.0030	0.0030	0.0030	0.0100	0.0500	0.150
propyl acetate	None	None	None	None	None	None	None	None	None	None	None	None	None	None	None	None	0.0010	0.0007	0.0007	0.0007	0.0007
ethyl isobutyrate	None	None	None	None	None	None	None	None	None	None	None	None	None	None	None	None	0.0010	0.0007	0.0007	0.0007	0.0007
ethyl hexanoate	None	None	None	None	None	None	None	None	None	None	None	None	None	None	None	None	0.0010	0.0007	0.0007	0.0007	0.0007
isovaleric acid, butyl ester	None	None	None	None	None	None	None	None	None	None	None	None	None	None	None	None	None	None	0.0007	0.0007	0.0007
ethyl octanoate	None	None	None	None	None	None	None	None	None	None	None	None	None	None	None	None	0.0010	0.0007	0.0007	0.0007	0.0007
ethyl decanoate	None	None	None	None	None	None	None	None	None	None	None	None	None	None	None	None	0.0010	0.0007	0.0007	0.0007	0.0007
ethyl laurate	None	None	None	None	None	None	None	None	None	None	None	None	None	None	None	None	0.0010	0.0007	0.0007	0.0007	0.0007

1110   The percent composition (v/v) of the metabolite mixtures used in fig. S1

51

References

1. **Mcfall-Ngai M**, **Hadfield MG**, **Bosch TCG**, **Carey HV**, **Domazet-Loso T**, **Douglas AE**, **Dubilier N**, **Eberl G**, **Fukami T**, **Gilbert SF**, **Hentschel U**, **King N**, **Kjelleberg S**, **Knoll AH**, **Kremer N**, **Mazmanian SK**, **Metcalf JL**, **Nealson K**, **Pierce NE**, **Rawls JF**, **Reid A**, **Ruby EG**, **Rumpho M**, **Sanders JG**, **Tautz D**, **Wernegreen JJ**. 2013. Animals in a bacterial world, a new imperative for the life sciences. PNAS **110**:3229–3236.

2. **van Nood E**, **Vrieze A**, **Nieuwdorp M**, **Fuentes S**, **Zoetendal EG**, **de Vos WM**, **Visser CE**, **Kuijper EJ**, **Bartelsman JFWM**, **Tijssen JGP**, **Speelman P**, **Dijkgraaf MGW**, **Keller JJ**. 2013. Duodenal infusion of donor feces for recurrent *Clostridium difficile*. N Engl J Med **368**:407–415.

3. **Zhu L**, **Wu Q**, **Dai J**, **Zhang S**, **Wei F**. 2011. Evidence of cellulose metabolism by the giant panda gut microbiome. PNAS **108**:17714–17719.

4. **Degnan PH**, **Taga ME**, **Goodman AL**. 2014. Vitamin B12 as a modulator of gut microbial ecology. Cell Metab **20**:769–778.

5. **Bravo JA**, **Forsythe P**, **Chew MV**, **Escaravage E**, **Savignac HM**, **Dinan TG**, **Bienenstock J**, **Cryan JF**. 2011. Ingestion of Lactobacillus strain regulates emotional behavior and central GABA receptor expression in a mouse via the vagus nerve. PNAS **108**:16050–16055.

6. **Rath CM**, **Dorrestein PC**. 2012. The bacterial chemical repertoire mediates metabolic exchange within gut microbiomes. Curr Opin Microbiol **15**:147–154.

7. **Manor O**, **Levy R**, **Borenstein E**. 2014. Mapping the inner workings of the microbiome: genomic- and metagenomic-based study of metabolism and metabolic interactions in the human microbiome. Cell Metab **20**:742–752.

8. **Gerber GK**. 2014. The dynamic microbiome. FEBS Letters **588**:4131–4139.

9. **Gonzalez A**, **King A**, **Robeson MS**, **Song S**, **Shade A**, **Metcalf JL**, **Knight R**. 2012. Characterizing microbial communities through space and time. Current Opinion in Biotechnology **23**:431–436.

10. **Derewacz DK**, **Covington BC**, **McLean JA**, **Bachmann BO**. 2015. Mapping microbial response metabolomes for induced natural product discovery. ACS chemical biology **10**:1998–2006.

11. **Goh E-B**, **Yim G**, **Tsui W**, **McClure J**, **Surette MG**, **Davies J**. 2002. Transcriptional modulation of bacterial gene expression by subinhibitory concentrations of antibiotics. PNAS **99**:17025–17030.

12. **Ridaura VK**, **Faith JJ**, **Rey FE**, **Cheng J**, **Duncan AE**, **Kau AL**, **Griffin NW**, **Lombard V**, **Henrissat B**, **Bain JR**, **Muehlbauer MJ**, **Ilkayeva O**, **Semenkovich CF**, **Funai K**, **Hayashi DK**, **Lyle BJ**, **Martini MC**, **Ursell LK**, **Clemente JC**, **Van Treuren W**, **Walters WA**, **Knight R**, **Newgard CB**, **Heath AC**, **Gordon JI**. 2013. Gut microbiota from twins discordant for obesity modulate metabolism in mice. Science **341**:1241214.

13. **Costello EK**, **Lauber CL**, **Hamady M**, **Fierer N**, **Gordon JI**, **Knight R**. 2009. Bacterial community variation in human body habitats across space and time. Science **326**:1694–1697.

14. **Ivanov II**, **Atarashi K**, **Manel N**, **Brodie EL**, **Shima T**, **Karaoz U**, **Wei D**, **Goldfarb KC**, **Santee CA**, **Lynch SV**, **Tanoue T**, **Imaoka A**, **Itoh K**, **Takeda K**, **Umesaki Y**, **Honda K**, **Littman DR**. 2009. Induction of intestinal Th17 cells by segmented filamentous bacteria. Cell **139**:485–498.

1150 15. **Poulsen M**, **Hu H**, **Li C**, **Chen Z**, **Xu L**, **Otani S**, **Nygaard S**, **Nobre T**, **Klaubauf S**, **Schindler**
1151   **PM**, **Hauser F**, **Pan H**, **Yang Z**, **Sonnenberg ASM**, **de Beer ZW**, **Zhang Y**, **Wingfield MJ**,
1152   **Grimmelikhuijzen CJP**, **de Vries RP**, **Korb J**, **Aanen DK**, **Wang J**, **Boomsma JJ**, **Zhang G**.
1153   2014. Complementary symbiont contributions to plant decomposition in a fungus-farming termite.
1154   PNAS **111**:14500–14505.

1155 16. **Rakoff-Nahoum S**, **Coyne MJ**, **Comstock LE**. 2014. An ecological network of polysaccharide
1156   utilization among human intestinal symbionts. Current Biology **24**:40–49.

1157 17. **Rakoff-Nahoum S**, **Foster KR**, **Comstock LE**. 2016. The evolution of cooperation within the gut
1158   microbiota. Nature **533**:255–259.

1159 18. **Fraune S**, **Anton-Erxleben F**, **Augustin R**, **Franzenburg S**, **Knop M**, **Schröder K**, **Willoweit-**
1160   **Ohl D**, **Bosch TC**. 2015. Bacteria-bacteria interactions within the microbiota of the ancestral
1161   metazoan *Hydra* contribute to fungal resistance. ISME J **9**:1543–1556.

1162 19. **Chandler JA**, **Lang JM**, **Bhatnagar S**, **Eisen JA**, **Kopp A**. 2011. Bacterial communities of diverse
1163   *Drosophila* species: ecological context of a host–microbe model system. PLoS Genet **7**:e1002272.

1164 20. **Chandler JA**, **Eisen JA**, **Kopp A**. 2012. Yeast communities of diverse *Drosophila* species:
1165   comparison of two symbiont groups in the same hosts. Applied and Environmental Microbiology
1166   **78**:7327–7336.

1167 21. **Broderick NA**, **Lemaitre B**. 2012. Gut-associated microbes of *Drosophila melanogaster*. Gut
1168   Microbes **3**:307–321.

1169 22. **Camargo R**, **Phaff HJ**. 1957. Yeasts occurring in *Drosophila* flies and in fermenting tomato fruits
1170   in northern California. J Food Science **22**:367–372.

1171 23. **Barata A**, **Malfeito-Ferreira M**, **Loureiro V**. 2012. The microbial ecology of wine grape berries. Int
1172   J Food Microbiol **153**:243–259.

1173 24. **Erkosar B**, **Storelli G**, **Defaye A**, **Leulier F**. 2013. Host-intestinal microbiota mutualism: "learning
1174   on the fly". Cell Host & Microbe **13**:8–14.

1175 25. **Blum JE**, **Fischer CN**, **Miles J**, **Handelsman J**. 2013. Frequent replenishment sustains the
1176   beneficial microbiome of *Drosophila melanogaster*. MBio **4**:e00860–13.

1177 26. **Broderick NA**, **Buchon N**, **Lemaitre B**. 2014. Microbiota-induced changes in *Drosophila*
1178   *melanogaster* host gene expression and gut morphology. MBio **5**:e01117–14.

1179 27. **Becher PG**, **Flick G**, **Rozpędowska E**, **Schmidt A**, **Hagman A**, **Lebreton S**, **Larsson MC**,
1180   **Hansson BS**, **Piškur J**, **Witzgall P**, **Bengtsson M**. 2012. Yeast, not fruit volatiles mediate
1181   *Drosophila melanogaster* attraction, oviposition and development. Functional Ecology **26**:822–828.

1182 28. **Christiaens JF**, **Franco LM**, **Cools TL**, **De Meester L**, **Michiels J**, **Wenseleers T**, **Hassan BA**,
1183   **Yaksi E**, **Verstrepen KJ**. 2014. The fungal aroma gene *ATF1* promotes dispersal of yeast cells
1184   through insect vectors. Cell Rep **9**:425–432.

1185 29. **Schiabor KM**, **Quan AS**, **Eisen MB**. 2014. *Saccharomyces cerevisiae* mitochondria are required
1186   for optimal attractiveness to *Drosophila melanogaster*. PLoS ONE **9**:e113899.

1187 30. **Palanca L**, **Gaskett AC**, **Günther CS**, **Newcomb RD**, **Goddard MR**. 2013. Quantifying variation

1188   in the ability of yeasts to attract *Drosophila melanogaster*. PLoS ONE **8**:e75332.

1189   31.   **Venu I**, **Durisko Z**, **Xu J**, **Dukas R**. 2014. Social attraction mediated by fruit flies' microbiome. J
1190   Exp Biol **217**:1346–1352.

1191   32.   **Ai M**, **Min S**, **Grosjean Y**, **Leblanc C**, **Bell R**, **Benton R**, **Suh GSB**. 2010. Acid sensing by the
1192   *Drosophila* olfactory system. Nature **468**:691–695.

1193   33.   **Wong CNA**, **Ng P**, **Douglas AE**. 2011. Low-diversity bacterial community in the gut of the fruitfly
1194   *Drosophila melanogaster*. Environ Microbiol **13**:1889–1900.

1195   34.   **Shin SC**, **Kim S-H**, **You H**, **Kim B**, **Kim AC**, **Lee K-A**, **Yoon J-H**, **Ryu J-H**, **Lee W-J**. 2011.
1196   *Drosophila* microbiome modulates host developmental and metabolic homeostasis via insulin
1197   signaling. Science **334**:670–674.

1198   35.   **Storelli G**, **Defaye A**, **Erkosar B**, **Hols P**, **Royet J**, **Leulier F**. 2011. *Lactobacillus plantarum*
1199   promotes *Drosophila* systemic growth by modulating hormonal signals through TOR-dependent
1200   nutrient sensing. Cell Metab **14**:403–414.

1201   36.   **Buchon N**, **Broderick NA**, **Chakrabarti S**, **Lemaitre B**. 2009. Invasive and indigenous microbiota
1202   impact intestinal stem cell activity through multiple pathways in *Drosophila*. Genes Dev **23**:2333–
1203   2344.

1204   37.   **Newell PD**, **Douglas AE**. 2014. Interspecies interactions determine the impact of the gut
1205   microbiota on nutrient allocation in *Drosophila melanogaster*. Applied and Environmental
1206   Microbiology **80**:788–796.

1207   38.   **Wong AC-N**, **Dobson AJ**, **Douglas AE**. 2014. Gut microbiota dictates the metabolic response of
1208   *Drosophila* to diet. J Exp Biol **217**:1894–1901.

1209   39.   **El-Zoghbi M**. 1994. Biochemical changes in some tropical fruits during ripening. Food Chem
1210   **49**:33–37.

1211   40.   **Abu-Goukh A-BA**, **Bashir HA**. 2003. Changes in pectic enzymes and cellulase activity during
1212   guava fruit ripening. Food Chem **83**:213–218.

1213   41.   **Mao WW**, **Kinsella JE**. 1981. Amylase activity in banana fruit: properties and changes in activity
1214   with ripening. J Food Science **46**:1400–1403.

1215   42.   **Barbe JC**, **De Revel G**, **Joyeux A**, **Bertrand A**, **Lonvaud-Funel A**. 2001. Role of botrytized
1216   grape micro-organisms in SO2 binding phenomena. J Appl Microbiol **90**:34–42.

1217   43.   **Turner SL**, **Ray A**. 2009. Modification of CO2 avoidance behaviour in *Drosophila* by inhibitory
1218   odorants. Nature **461**:277–281.

1219   44.   **Anagnostou C**, **Dorsch M**, **Rohlfs M**. 2010. Influence of dietary yeasts on *Drosophila
1220   melanogaster* life-history traits. Entomologia Experimentalis et Applicata **136**:1–11.

1221   45.   **Abuin L**, **Bargeton B**, **Ulbrich MH**, **Isacoff EY**, **Kellenberger S**, **Benton R**. 2011. Functional
1222   architecture of olfactory ionotropic glutamate receptors. Neuron **69**:44–60.

1223   46.   **Hallem EA**, **Carlson JR**. 2006. Coding of odors by a receptor repertoire. Cell **125**:143–160.

1224 47. **Larsson MC**, **Domingos AI**, **Jones WD**, **Chiappe ME**, **Amrein H**, **Vosshall LB**. 2004. *Or83b*
1225   encodes a broadly expressed odorant receptor essential for *Drosophila* olfaction. Neuron **43**:703–
1226   714.

1227 48. **Mathew D**, **Martelli C**, **Kelley-Swift E**, **Brusalis C**, **Gershow M**, **Samuel ADT**, **Emonet T**,
1228   **Carlson JR**. 2013. Functional diversity among sensory receptors in a *Drosophila* olfactory circuit.
1229   PNAS **110**:E2134–43.

1230 49. **Asahina K**, **Louis M**, **Piccinotti S**, **Vosshall LB**. 2009. A circuit supporting concentration-
1231   invariant odor perception in *Drosophila*. Journal of Biology **8**:1–19.

1232 50. **Stökl J**, **Strutz A**, **Dafni A**, **Svatos A**, **Doubsky J**, **Knaden M**, **Sachse S**, **Hansson BS**,
1233   **Stensmyr MC**. 2010. A deceptive pollination system targeting Drosophilids through olfactory
1234   mimicry of yeast. Current Biology **20**:1846–1852.

1235 51. **Semmelhack JL**, **Wang JW**. 2009. Select *Drosophila* glomeruli mediate innate olfactory attraction
1236   and aversion. Nature **459**:218–223.

1237 52. **Linda F Chuang EBC**. 1968. Biosynthesis of diacetyl in bacteria and yeast. J Bacteriol **95**:2083–
1238   2089.

1239 53. **Ruyters S**, **Mukherjee V**, **Verstrepen KJ**, **Thevelein JM**, **Willems KA**, **Lievens B**. 2015.
1240   Assessing the potential of wild yeasts for bioethanol production. J Ind Microbiol Biotechnol **42**:39–
1241   48.

1242 54. **Ranganathan S**, **Davis DG**, **Hood RD**. 1987. Developmental toxicity of ethanol in *Drosophila*
1243   *melanogaster*. Teratology **36**:45–49.

1244 55. **Azanchi R**, **Kaun KR**, **Heberlein U**. 2013. Competing dopamine neurons drive oviposition choice
1245   for ethanol in *Drosophila*. PNAS **110**:21153–21158.

1246 56. **Kacsoh BZ**, **Lynch ZR**, **Mortimer NT**, **Schlenke TA**. 2013. Fruit flies medicate offspring after
1247   seeing parasites. Science **339**:947–950.

1248 57. **Lhocine N**, **Ribeiro PS**, **Buchon N**, **Wepf A**, **Wilson R**, **Tenev T**, **Lemaitre B**, **Gstaiger M**, **Meier**
1249   **P**, **Leulier F**. 2008. PIMS modulates immune tolerance by negatively regulating *Drosophila* innate
1250   immune signaling. Cell Host & Microbe **4**:147–158.

1251 58. **Ryu J-H**, **Kim S-H**, **Lee H-Y**, **Bai JY**, **Nam Y-D**, **Bae J-W**, **Lee DG**, **Shin SC**, **Ha E-M**, **Lee W-J**.
1252   2008. Innate immune homeostasis by the homeobox gene caudal and commensal-gut mutualism
1253   in *Drosophila*. Science **319**:777–782.

1254 59. **Paredes JC**, **Welchman DP**, **Poidevin M**, **Lemaitre B**. 2011. Negative regulation by amidase
1255   PGRPs shapes the *Drosophila* antibacterial response and protects the fly from innocuous
1256   infection. Immunity **35**:770–779.

1257 60. **Costechareyre D**, **Capo F**, **Fabre A**, **Chaduli D**, **Kellenberger C**, **Roussel A**, **Charroux B**,
1258   **Royet J**. 2016. Tissue-specific regulation of *Drosophila* NF-KB pathway activation by
1259   peptidoglycan recognition protein SC. J Innate Immun **8**:67–80.

1260 61. **Broderick NA**. 2016. Friend, foe or food? Recognition and the role of antimicrobial peptides in gut
1261   immunity and *Drosophila*-microbe interactions. Philos Trans R Soc Lond, B, Biol Sci
1262   **371**:20150295.

1263   62.   **Piper MDW**, **Blanc E**, **Leitão-Gonçalves R**, **Yang M**, **He X**, **Linford NJ**, **Hoddinott MP**, **Hopfen**
1264   **C**, **Soultoukis GA**, **Niemeyer C**, **Kerr F**, **Pletcher SD**, **Ribeiro C**, **Partridge L**. 2014. A holidic
1265   medium for *Drosophila melanogaster*. Nat Methods **11**:100–105.

1266   63.   **Jarosz DF**, **Brown JCS**, **Walker GA**, **Datta MS**, **Ung WL**, **Lancaster AK**, **Rotem A**, **Chang A**,
1267   **Newby GA**, **Weitz DA**, **Bisson LF**, **Lindquist S**. 2014. Cross-kingdom chemical communication
1268   drives a heritable, mutually beneficial prion-based transformation of metabolism. Cell **158**:1083–
1269   1093.

1270   64.   **Staubach F**, **Baines JF**, **Künzel S**, **Bik EM**, **Petrov DA**. 2013. Host species and environmental
1271   effects on bacterial communities associated with *Drosophila* in the laboratory and in the natural
1272   environment. PLoS ONE **8**:e70749.

1273   65.   **Callejón RM**, **González AG**, **Troncoso AM**, **Morales ML**. 2008. Optimization and validation of
1274   headspace sorptive extraction for the analysis of volatile compounds in wine vinegars. Journal of
1275   Chromatography A **1204**:93–103.

1276   66.   **Xiao Z**, **Dai S**, **Niu Y**, **Yu H**, **Zhu J**, **Tian H**, **Gu Y**. 2011. Discrimination of chinese vinegars based
1277   on headspace solid-phase microextraction-gas chromatography mass spectrometry of volatile
1278   compounds and multivariate analysis. J Food Science **76**:1125–1135.

1279   67.   **Joseph RM**, **Devineni AV**, **King IFG**, **Heberlein U**. 2009. Oviposition preference for and
1280   positional avoidance of acetic acid provide a model for competing behavioral drives in *Drosophila*.
1281   PNAS **106**:11352–11357.

1282

1283